1290

UNIVERSIDADE Ð COIMBRA

Maria Francisca Pires Gonçalves

PHOTOCATALYTIC PROCESSES OPTIMIZATION USING SUPPORTED TIO2 TO OXIDIZE POLLUTANTS IN LIQUID EFFLUENTS

September 2022

Faculty of Science and Technology of the University of Coimbra

Photocatalytic processes optimization using supported TiO$_2$ to oxidize pollutants in liquid effluents

Maria Francisca Pires Gonçalves

Coimbra, September 2022

1 2 9 0

UNIVERSIDADE Ð
COIMBRA

"The more I study, the more insatiable do I feel my genius for it to be."

Ada Lovelace

Acknowledgments

To write the acknowledgments, it only makes sense for me to write them in my native language, Portuguese, so it will be written that way.

A realização desta dissertação foi uma jornada que permitiu um crescimento, não só a nível académico, mas também a nível pessoal. Foram vários os percalços ao longo do tempo, mas graças a várias pessoas, foi possível ultrapassá-los.

Queria agradecer em primeiro lugar à Doutora Margarida Quina pelos conselhos e pela preocupação demonstrada ao longo deste caminho. Agradeço imenso pelo encorajamento para prosseguir com este projeto. Em seguida, ao Doutor João Gomes, por todas as ideias e dicas que permitiram avançar com os ensaios realizados. Obrigada pela paciência e prontidão em tirar qualquer dúvida que mais me atormentava.

Aos meus colegas de laboratório, Francisco Brandão, Mariana Alvim, Telma Vaz, Eva Gomes e Vittorina Rocha por fazerem com que o ambiente fosse bastante agradável e especial. Ao Sadjo Danfá, que me ajudou bastante na preparação do fotocatalisador, um grande obrigada. Obrigada às minhas colegas Joana Martins e Rita Brites, pelo companheirismo e por todas as palavras de força quando mais precisei de as ouvir. Obrigada por tudo.

Aos meus amigos, em especial à Anita, Andreia, Isabel, Eduardo, Filipa, Patrícia, Ana e Inês por todo o apoio que me demonstraram ao longo deste curso e por nunca me deixarem desanimar quando me sentia mais em baixo. Desculpem por todas as ausências, serão compensadas da melhor maneira.

Por último, mas não menos importante, queria agradecer do fundo do meu coração, à minha família, em especial à minha mãe, Ana Paula e ao meu avô Basílio. Sem vocês, não poderia ter ingressado neste curso e ter alcançado todos as grandezas. Obrigada por nunca me deixarem desistir e por sofrerem comigo todos os momentos menos felizes desta caminhada. À minha irmã Sofia, por ser uma inspiração para mim todos os dias, por me ensinar a lutar por aquilo que se quer realmente. Muito obrigada aos três. Serão sempre o meu exemplo.

Abstract

The great variety of pharmaceuticals available for human and veterinary consumption is considered a health advance, but their expelling into water bodies is a matter of concern. These compounds negatively impact the environment, since the wastewater treatment plants (WWTPs) are not efficient for the removal of such components due to the refractory character, and it is necessary to use a suitable technology. In this sense, advanced oxidation processes (AOPs) such as photocatalytic oxidation appear as a suitable alternative.

The main objective of this thesis is to promote sulfamethoxazole (SMX) degradation using TiO_2 supported in a ceramic material called LECA as a photocatalyst. This choice comes from the difficulty of recovering TiO_2 as a powder due to the nanoparticle size, although it is relevant to retain the efficiency when the support is used. Two different reactor configurations were used, a slurry reactor and a fixed bed reactor. Several parameters were tested, such as the amount of photocatalyst, and mixing type, to understand which were the best results for the SMX degradation. The first step was to produce the photocatalyst supported in LECA, where were used two concentrations of TiO_2 suspension, 3.6% (w/w) and 5% (w/w), impregnated in LECA.

The impact of the photocatalyst amount reveals that the increase in the dosage improves the SMX degradation, reaching about 53.5% when using UV-A radiation and aeration for the higher amount of photocatalyst. After selecting the best dosage, the effect of the reactor layout was studied. Two different contact types, aeration and a magnetic stirrer were tested for the slurry reactor. The magnetic stirrer had the best results in terms of SMX degradation but had higher loss of TiO_2 nanoparticles for the liquid solution. Therefore, aeration is considered a better option to promote the mixing of the reactional medium. The radiation type, solar and UV-A radiation, was compared for both reactor configurations. For 120 min of reaction time, the slurry reactor reached about 92% of SMX degradation (5% (w/w) of TiO_2 impregnated in LECA), and the fixed bed reactor, for the same time and photocatalyst amount, reached 69% of degradation. Following these effects, it was also tested the photocatalyst distribution mode for the fixed bed reactor. The results were considered similar, around 75% to 80% of removal. Lastly, the recirculation rate was compared for the fixed bed reactor, leading to 91.5% of SMX elimination when the lower flowrate (0.006 L min^{-1}) was used for the same total reaction time. The TiO_2 loss during the fixed bed tests was similar to each other, which was around 20%. When the reuse of the photocatalyst was tested for the fixed bed reactor after three cycles, the efficiency decreased by 6% at the end of the third cycle.

In summary, the two-reactor configuration has advantages and disadvantages, but in terms of SMX degradation rates, the slurry reactor for the conditions tested had the best results.

Resumo

A grande variedade de produtos farmacêuticos disponíveis para consumo humano e veterinário é considerada um avanço na saúde, mas a sua excreção para a água deve merecer uma especial atenção. Estes compostos têm um impacto negativo no ambiente, uma vez que as estações de tratamento de águas residuais (ETAR) não são eficientes para a remoção de tais componentes devido ao carácter refratário, sendo necessário utilizar uma tecnologia adequada. Neste sentido, os processos avançados de oxidação, tais como a oxidação fotocatalítica, surgem como uma alternativa aos métodos tradicionais.

O principal objetivo deste estudo é promover a degradação do sulfamethoxazole (SMX) usando TiO_2 suportado num material cerâmico, LECA, como fotocatalisador. Esta escolha vem da dificuldade em recuperar o TiO_2 como pó, devido ao tamanho das nanopartículas, embora seja relevante manter a eficiência quando o suporte é utilizado. Foram utilizadas duas configurações diferentes de reatores, um *slurry* e um reator de leito fixo. Foram avaliados vários parâmetros, tais como a quantidade de fotocatalisador ou a mistura na solução, a fim de compreender quais as melhores condições para a degradação do SMX. O primeiro passo foi produzir o fotocatalisador suportado em LECA, onde foram utilizadas duas concentrações de suspensão de TiO_2, 3,6% (m/m) e 5% (m/m), impregnadas em LECA.

O impacto da quantidade de fotocatalisador revela que o aumento da dose melhora a degradação SMX, atingindo cerca de 53,5% quando se utiliza uma radiação UV-A e borbulhamento, para a quantidade maior de fotocatalisador. Após a seleção da melhor dosagem, foi estudado o efeito do *layout* do reator. Dois tipos diferentes de contacto, borbulhamento e um agitador magnético foram testados para o reator *slurry*. O agitador magnético teve os melhores resultados em termos de degradação SMX, mas teve uma maior libertação de nanopartículas de TiO_2 para a solução líquida. Portanto o borbulhamento é considerado a melhor opção para promover a mistura do meio reacional. O tipo de radiação, solar e radiação UV-A, foi comparado para ambas as configurações de reatores. Durante 120 min de reação, o reator *slurry* atingiu cerca de 92% de degradação SMX (5% (m/m) de TiO_2 impregnado em LECA), e o reator de leito fixo, durante o mesmo tempo e a mesma quantidade de fotocatalisador, atingiu 69% de degradação. Após estes efeitos, foi também testado o modo de distribuição do fotocatalisador para o reator de leito fixo. Os resultados foram considerados semelhantes, cerca de 75% a 80% da remoção. Finalmente, o caudal de recirculação foi comparado para o reator de leito fixo, eliminando 91,5% SMX quando o fluxo foi mais baixo (0,006 L min^{-1}) para o mesmo tempo total de reação. A perda de TiO_2 durante a reação do leito

fixo foi semelhante entre si, que foi de cerca de 20%. Quando a reutilização do fotocatalisador foi testada para o reator de leito fixo após três ciclos e a eficiência diminuiu 6% no final do terceiro ciclo.

Em resumo, a configuração dos dois reatores tem vantagens e desvantagens, mas em termos de taxas de degradação SMX, o reator *slurry* para as condições testadas teve os melhores resultados.

Palavras-chave: Fotocatálise, Sulfamethoxazole, Dióxido de titânio, LECA, Reator *Slurry*, Reator de Leito Fixo, *Layout* do reator, Reutilização do fotocatalisador

Index

List of Figures

List of Tables

Symbols

ε_v – volumetric porosity

μ - fluid viscosity (Pa s)

3.6%TiO$_2$/LECA – 3.6% (w/w) of TiO$_2$ impregnated in LECA

5%TiO$_2$/LECA – 5% (w/w) of TiO$_2$ impregnated in LECA

A – surface area (m^2)

C – Concentration (mg L^{-1})

C$_0$ – Initial concentration of the pollutant (mg L^{-1})

C$_1$ – Configuration with all the particles

C$_2$ – Configuration with half of particles at the beginning of the column and filling upper it

C$_3$ – Configuration with half of the particles between the filling

C$_4$ – Configuration with half of the particles in layers with the filling

d – column diameter (m)

e$^-$ - Electron

E$_g$ – Energy band gap

eV – Electron volt

h$^+$ - Holes

hν – Incident radiation energy

K – Equilibrium adsorption constant (L mg^{-1})

k – Reaction rate constant (min^{-1})

k$_{ap}$ – Kinetic constant of pseudo-first order reaction (min^{-1})

m$_f$ - Final mass (g)

m$_i$ – Initial mass (g)

m$_{TiO2incorporated}$ – TiO$_2$ incorporated in LECA (g)

Q – Circulation feed (m^3 s^{-1})

Re – Reynolds number

t – Reaction time (min)

TiO$_2$ - Titanium Dioxide

u$_I$ – Interstitial velocity (m s^{-1})

ρ - Density (kg m^{-3})

Abbreviations

AMI – 3-amino-5-methylisoxazole

AOP – Advanced oxidation processes

API – Active pharmaceutical ingredient

ASW – Artificial sweeteners

BZQ – p-benzoquinone

CB – Conduction band

CBZ – Carbendazim

CEC – Contaminants of emerging concerns

EDC – Endocrine-disrupting compounds

FR- Flame retardants

HPLC – High- performance liquid chromatography

LECA – Lightweight expanded clay aggregate

MCP – Monocrotophos

OM – Organic molecules

OXL – Oxalic acid

OXM – Oxamic acid

PPCP – Pharmaceuticals and care products

RAS – Recirculation aquaculture system

rpm – Rotations per minute

SMX – Sulfamethoxazole

SNA – Sulfanilic acid

TMP – Trimethoprim

UV – Ultraviolet radiation

UV-A Ultraviolet radiation with wavelength between (320-400 nm)

UV-B – Ultraviolet radiation with wavelength between (290-320 nm)

VB – Valance band

WWTP – Wastewater treatment plant

1. Introduction

1.1   Scope and Motivation

It is a well-known fact that water is one of the most important resources on Earth. Every living being requires water to live, and it is easy to get dehydrated and consequently die. (Chaplin, 2001).

Even though freshwater is widely consumed in many activities, many countries are under water stress. Its amount in nature is controlled by the hydrological cycle, and human activities have an important role in it (Stanhill, 1986). With population growth reaching unprecedented numbers, sectors like agriculture, domestic and industrial are also increasing their water demand (Zimmerman et al., 2008). It is estimated that four billion people suffer from water scarcity at least one month per year, and 1.6 billion do not have the means to reach water (Sarni & Grant, 2021). Other important factors regarding freshwater decrease are climate change and water contamination. (VO et al., 2014; Long et al., 2020).

It is expected that all regions around the globe are or will experience the negative impacts of climate change with a negative impact on water resources and freshwater availability (Abbaspour et al., 2009). Climate change creates uncertainty regarding water supply, due to the impact on the environment. It rises seasonal variability, with an unprecedented increase in water-stressed areas and growths more water-stressed places that were not experiencing this phenomenon yet (Sarni & Grant, 2021).

Many water bodies are being contaminated, which decreases the availability and quality of freshwater around the world (Gorde & Jadhav, 2013; Sharma & Bhattacharya, 2017). It is estimated that 80% of industrial and municipal wastewater is discharged into the environment without any type of treatment, affecting not only human health but also ecosystems (Sarni & Grant, 2021).

Water pollution is increasing with a great variety of substances called contaminants of emerging concerns (CECs), which can be pharmaceuticals and care products (PPCPs), flame retardants (FRs), endocrine-disrupting compounds (EDCs), artificial sweeteners (ASWs), and pesticides (Salimi et al., 2017). These compounds are found in trace concentrations, ranging from nanograms per liter, up to milligrams per liter (Danfá et al., 2021; Salimi et al., 2017).

From all kinds of contaminants, pharmaceuticals are getting more attention in the last recent years, due to their negative impact on water bodies (Bottoni et al., 2010). More than 200 pharmaceuticals were detected in river water, and they are considered a huge danger due to their high solubility in water and poor degradation (Prasannamedha & Kumar, 2020). The presence of pharmaceuticals is mainly associated with emissions from the pharmaceutical

industry, hospitals, and houses where personal products and therapeutic drugs are consumed (Rivera-Utrilla et al., 2013).

The most prescribed type of drug in the world is antibiotics, and their consumption increased by 65% between 2000 and 2005 (Balasubramanian et al., 2021). It is predicted that, if no alterations in policies occur and the rate of consumption stays constant, antibiotic consumption worldwide will increase by 15% in 2030 (Prasannamedha & Kumar, 2020). This kind of pharmaceutical (antibiotics) is also known as CEC, because its concentration is getting higher than it should, and can impact negatively the environment, aquatic life, and humans (Baralla et al., 2021). Since antibiotics are not totally metabolized in the body, a considerable fraction is discharged into water bodies, and thus antibiotics are considered a priority in terms of research (Bottoni et al., 2010; Johnson et al., 2015). These contaminants can generate resistant bacteria, allowing them to survive and become harmful to the environment (Jendrzejewska & Karwowska, 2018).

In Portugal, the most detected antibiotics in wastewater are quinolones, tetracyclines, and sulfonamides (Carvalho & Santos, 2016). Sulfamethoxazole (SMX) is listed in the top 30 prescribed antibiotics, and it is one of the most common sulfonamides prescribed in human medicine (Prasannamedha & Kumar, 2020). Approximately 15% of this type of antibiotic is expelled from the body and accumulates in wastewater. (Lester et al., 2010). Moreover, this antibiotic belongs to the list of substances to be monitored by the European Commission, where the maximum concentration allowance is 100 ng L^{-1} (Decision (EU) 2022/1307).

The drug excretion is discharged into ordinary wastewater treatment plants (WWTPs) that do not have great removal values of these antibiotics, because they are not biodegradable or adsorbed in the sewage sludge (Lester et al., 2010). For this reason, WWTP is the principal source of CEC, and pharmaceuticals released into the environment contaminants rivers, groundwater, and drinking water (Salimi et al., 2017).

To overcome these concerns, one of many options is treating wastewater with the advanced oxidation processes (AOPs), since it can produce reactive oxidative species capable to promote the refractory compounds abatement (VO et al., 2014). AOPs are recognized as the easiest and most practical technologies to degrade and increase the detoxification of WWTP effluents (Salimi et al., 2017). There are two types of AOPs: homogeneous system (for example, Fenton and Photo-Fenton systems and H_2O_2/UV) and heterogenous system (for example, photocatalysis) (Černigoj et al., 2007).

Photocatalysis (where the catalyst is a semiconductor) is an alternative technology to achieve higher degradation rates than conventional processes commonly used in WTTPs, becoming an effective way to remove organic pollutants such as CEC. This way, wastewater

can be treated to become a resource that can be reused or discharged safely into water bodies. (Černigoj et al., 2007). In this dissertation, heterogenous photocatalysis is the technology that is going to be studied, using solar and UV-A radiation and the semiconductor selected is titanium dioxide (TiO_2).

Titanium dioxide is one of the most studied catalysts because of its good properties compared to other semiconductors. It is non-expensive, safe, and stable, with great photocatalytic activity, and its usage in photocatalytic oxidation is considered the most viable alternative compared to other AOPs (Černigoj et al., 2007). Although TiO_2 as a powder (nanoparticles) is the most studied form in photocatalysis, in real applications supported TiO_2 is preferred due to the capacity of operating under continuous mode and capacity of being reused several times. However, it has the disadvantage of having a low area-to-volume ratio (Manassero et al., 2017; Danfá et al., 2021). This problem can be solved if used a proper reactor layout, which should maximize catalyst-illumination interaction and reduce mass transfer limitations (Manassero et al., 2017). The main reactor configurations are slurry reactors and fixed bed reactors.

For this reason, this thesis aims to study the reactor layout to increase the degradation of CECs, in particular SMX. Thus, different reactor configurations will be evaluated, as well as some variables such as radiation, catalyst quantity in the reaction, and flowrate.

1.2   Thesis Objectives

The present dissertation aims to give a contribution to the reactor layout for conducting photocatalytic oxidation using different types of radiation source. The compound used as an organic pollutant was SMX and TiO_2 was used as a semiconductor, supported in Lightweight Expanded Clay Aggregate (LECA). Several studies were made for this purpose, in particular, the analysis of:

  i.   the effect of the photocatalyst dosage in the reactor;
 ii.   the effect of mixing type;
iii.   the effect of different radiation sources;
 iv.   the effect of photocatalyst distribution in the reactor;
  v.   the effect of the recirculation rate;
 vi.   the photocatalyst reuse;
vii.   the reaction's by-products;

Indeed, the effect of the photocatalyst amount is studied to investigate which is the more suitable amount to better degrade the contaminant. The percentage of TiO_2 lost during the

reaction is also a parameter taken into account in the selection of the best dosage. Several studies were conducted using two different TiO_2 suspension concentrations, and further this concentration was evaluated in the same way as previously with the percentage of SMX removed and TiO_2 loss. The two different contact types are studied: mixing by a magnetic stirrer and aeration with an air pump. Different radiation sources were also tested, through the comparison results with UV-A and solar radiation. The fourth objective evaluates the efficiency of different photocatalyst distributions in the fixed bed reactor, to understand if the placement of the particles influences the results.

Moreover, the reuse of the catalyst is considered, to evaluate how many times can the same catalyst be used, without losing much efficiency. It is important to mention that these steps were made for different reactor configurations.

1.3   Thesis Organization

This dissertation is divided into six chapters. It begins with the first chapter, with an introduction, where the scope and motivation and the main objectives are described. Next, theoretical fundaments make up part of the second chapter, where some important definitions and concepts are mentioned. The third chapter is related to the state of the art, exposing some studies to compare with the results in this study. The materials and methods used throughout the study are all described in chapter four. Results and discussion are presented in chapter 5, where all the results obtained are discussed regarding the effect of the photocatalyst dosage in the reactor, all the parameters analyzed for all the reactor configurations, the photocatalyst reuse, and the by-products from the reactions. Lastly, chapter 6 has a summary of all the conclusions obtained and future work that can be made regarding the present study.

2. Theoretical Background

2.1   Contaminants of Emerging Concern in Wastewater

Several chemicals are considered CECs and they are characterized based on their chemical structure, toxicity, and negative impacts on living beings and the environment (Yadav et al., 2021). It is important to mention that the number of CECs is increasing continuously, as new compounds are being developed and used in all kinds of activities (Pastorino & Ginebreda, 2021). However, these compounds are not usually regulated in environmental legislation, which brings even more concern (Danfá et al., 2021).

Some of the deleterious effects of CECs are infertility, decrease in gamete production, and other reproductive problems, due to endocrine-disrupting chemicals (Yadav et al., 2021; Nilsen et al., 2019). According to Vidal-Dorsch et al. (2012), some CECs released to water bodies may accumulate into organisms (e.g. fish) and enter into the food chain. Exposure to low CECs concentrations may not cause severe toxicity effects but can change subtly aspects of the health and physiology of the organism. These can easily cause negative impacts on population levels and biodiversity (Nilsen et al., 2019). Other consequences of CECs exposure are the effects on the behavioral field of animals (e.g lack of aggressive behavior, change in mobility, and less ability to capture their prey) (Nilsen et al., 2019). CECs are emitted from several sources and can accumulate in the soil, water, and air, impacting negatively the environment and humans (Yadav et al., 2021). Since the effluents with these compounds are not efficiently treated due to limitations of primary and secondary treatments in WWTPs, these infrastructures are the major source of CECs in aquatic environments (Vidal-Dorsch et al., 2012). Disposal of industrial and urban waste may also originate contaminations with CECs in soil (Yadav et al., 2021).

Figure 1 shows the different pathways that the CECs can have, demonstrating that are several sources of these components, which contaminates all the sectors that consumes water. Therefore, if not treated properly, all sectors have the danger of using polluted water.
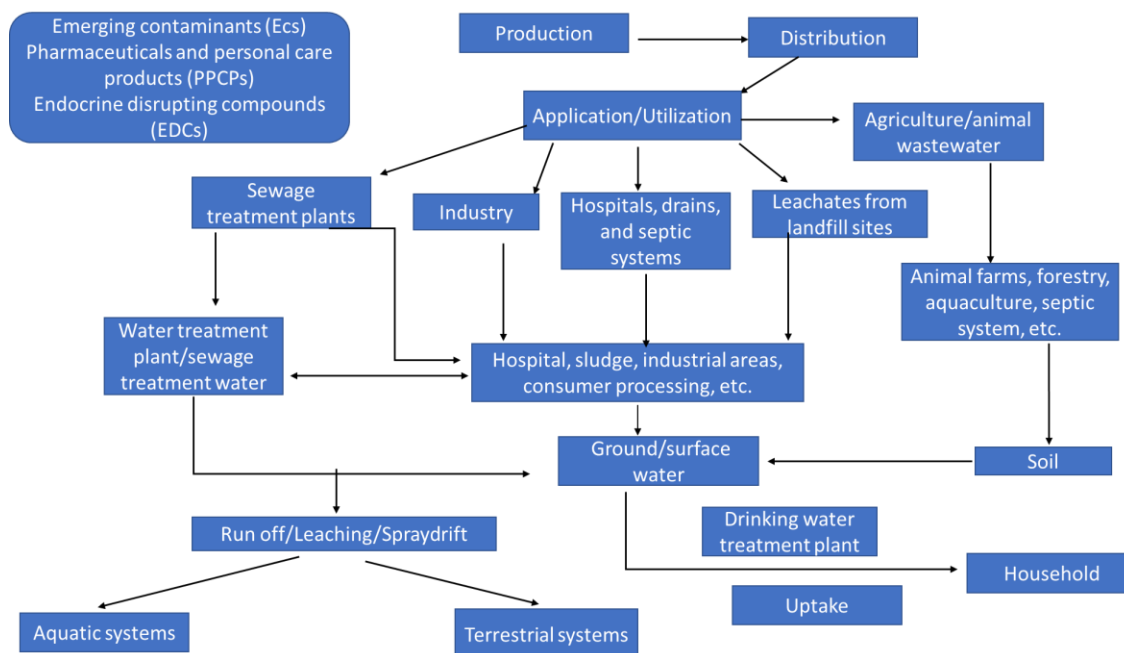
Figure 1. Contaminants of Emerging Concern (CECs) sources and where they can end up being (Adaptad from Yadav et al. 2021).
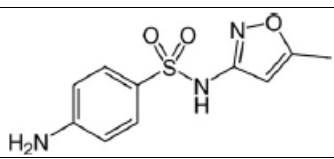
2.1.1 Sulfamethoxazole

Sulfamethoxazole is an antibiotic from the sulfonamide class, which is an inhibitor of the enzyme dihydropteroate synthase (Johnson et al., 2015). It is largely used due to its effective action against gram-negative and gram-positive bacteria, becoming a reference in the animal and food industry (Zdarta et al., 2022). For human health, it is used to cure respiratory tract, urinary tract, and enteric infections, and for veterinary use, sulfamethoxazole is found in herbicides and to treat and prevent diseases in aquaculture (Mestre & Carvalho, 2019).

SMX is usually associated with another active pharmaceutical ingredient (API), Trimethoprim (TMP), which is an antibiotic that belongs to the class of chemotherapeutic agents, that work as dihydrofolate reductase inhibitors (Johnson et al., 2015). This association turned into one medicine, co-trimoxazole, initially due to the development of antimicrobial resistance of older treatments and because it was much more efficient than SMX and TMP alone (Johnson et al., 2015). This drug has a SMX:TMP ratio of 5:1, allowing synergy between the two API (Johnson et al., 2015).

Table 1 summarizes the molecular structure and the chemical and physical properties of SMX, (Pubchem, 2022a; Mestre & Carvalho, 2019).
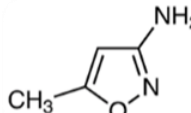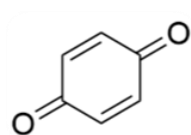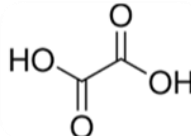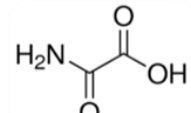
Table 1. Chemical and physical properties of SMX.

Properties of SMX	
Molecular formula	
IUPAC Name	4-amino-N-(5-methyl-1,2-oxazol-3-yl)benzenesulfonamide
Formula	$C_{10}H_{11}N_3O_3S$
Molecular Weight (Mw)	253.3 g mol^{-1}
Water Solubility (37ºC)	610 mg dm^{-3}

When SMX degradation occurs by photocatalysis, the concentration of SMX decreases, while other by-products can be generated. These by-products, final or intermediates, must be investigated with respect to their concentration and toxicity. Indeed, by-products from SMX degradation can decrease the degradation rate of the main compound, and even can be more toxic to aquatic species than the original compound (Dong et al., 2015).

There are some intermediates that can be formed in oxidizing reactions, such as 3-amino-5-methylisoxazole (AMI), p-benzoquinone (BZQ), oxalic acid (OXL) and oxamic acid (OXM) (Martini et al., 2019). Table 2 depicts the molecular formula of these compounds, their chemical formula, and molar mass.

Table 2. Chemical formula and molar mass of the by-products from SMX degradation.

Compound Name	Molecular Formula	Molar Mass (g mol^{-1})
AMI		98.10
BZQ		108.89
OXL		89.05
OXM		90.03

2.2   Technologies for CEC Treatment

To remove CECs from liquid effluents, there are three that are most used, recirculation aquaculture system (RAS), where physical filtration, anaerobic digestion, and UV disinfection are the main ones; biological method, being bioreactor, biofloc-technology and wetlands and phytoremediation included in it; and physicochemical procedure, which includes adsorption, AOPs and membranes separation technology (Ahmad et al., 2022). The technology used in the study of this dissertation is the AOP, which is going to be explained in detail.

2.2.1   Photocatalytic Processes

Among all the technologies that exist for CECs degradation, AOPs are considered a reliable solution to remove these contaminants since conventional WWTPs are inefficient to eliminate them. This process has the capacity of generating thermodynamically stable products, such as CO_2, H_2O, and other biodegradable organic compounds (Ameta et al., 2018).

AOPs use the oxidative potential of reactive oxygen species that have an unpaired electron, like hydroxyl radicals (•OH) or superoxide ($O_2^{\bullet-}$), generated from the reduction of water or oxygen molecules in water (Chirwa & Bamuza-Pemu, 2010; Ameta et al., 2018). Having an unpaired electron, radicals have short lifetimes, allowing them to react quickly with chemical species difficult to degrade through biological processes (Ameta et al., 2018).

According to the reactions regarding the mechanism of hydroxyl radical generation, there are several AOPs methods classified as can be seen in Figure 2 (Chirwa & Bamuza-Pemu, 2010). The AOP that is going to be described in this dissertation is photocatalysis, specifically with TiO_2 as a semiconductor.
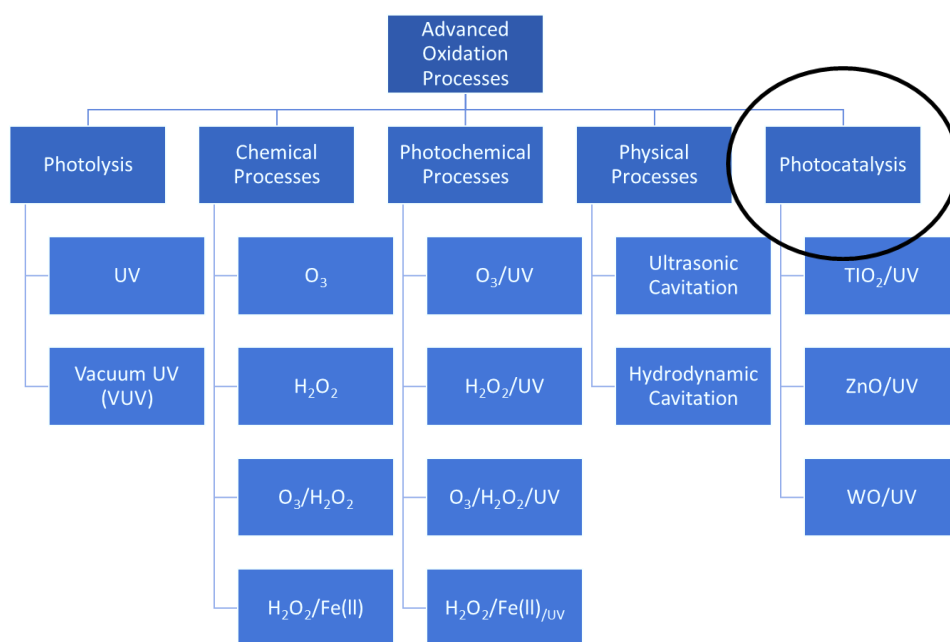
Figure 2. Classification of Advanced Oxidation Processes (AOPs), being photocatalysis one of the processes. Adapted from (Chirwa and Bamuza-Pemu 2010).

Photocatalysis is a process in which a reaction can only occur using radiation and a semiconductor. It is a widely used process because of its high degradation rates, high efficiency, and low-cost procedure (Long et al., 2020). The material that absorbs light is called a semiconductor, and the reactive oxidative species are produced when an electron-hole pair is generated by the semiconductor radiation exposure (Ameta et al., 2018).

There are two types of photocatalytic reactions, depending on the physical state of the reactants and photocatalyst. Homogenous photocatalysis occurs when the reactant and semiconductor are in the same physical phase, and heterogenous photocatalysis takes place when different phases are involved (Ameta et al., 2018). Photocatalysis is based on hydroxyl radicals production, which are very reactive and non-selective species, to completely degrade the compounds (pollutants) (Danfá et al., 2021). Heterogenous photocatalysis is the process considered in this dissertation, and thus described in more detail.

When the energy absorbed by the semiconductor is higher than the energy band gap (Eg), an electron (e-) can go from the valence band (VB) to the conduction band (CB). The Eg is the energy difference between the VB and CB. This value depends on the material that is used as a semiconductor. As electrons move from VB to CB, holes (h+) are formed, having an opposite direction from electrons. This motion generates an electrical current from the CB and to VB (Danfá et al., 2021; Monfort & Petrisková, 2021). When e-/h+ pairs are generated from incident irradiation energy (hv) equal to or higher than the Eg, reactive oxygen species are formed, which then can degrade the compound present in the effluents.

9

The photocatalytic mechanism is shown in Equations (1)-(7) and it is illustrated in Figure 3, where TiO_2 is applied as a semiconductor (Yasmina et al., 2014)

$$TiO_2 + hv \rightarrow TiO_2 + e_{CB}^- + h_{VB}^+ \tag{1}$$

$$O_2 + e_{CB}^- \rightarrow O_2^{\bullet -} \tag{2}$$

$$OM + e_{CB}^- \rightarrow reduction\ products \tag{3}$$

$$H_2O + h_{VB}^+ \rightarrow \bullet OH + H^+ \tag{4}$$

$$OH^- + h_{VB}^+ \rightarrow \bullet OH \tag{5}$$

$$OM + h_{VB}^+ \rightarrow oxidation\ products \tag{6}$$

$$\bullet OH + pollutants + O_2 \rightarrow CO_2 + H_2O + intermediate\ products \tag{7}$$
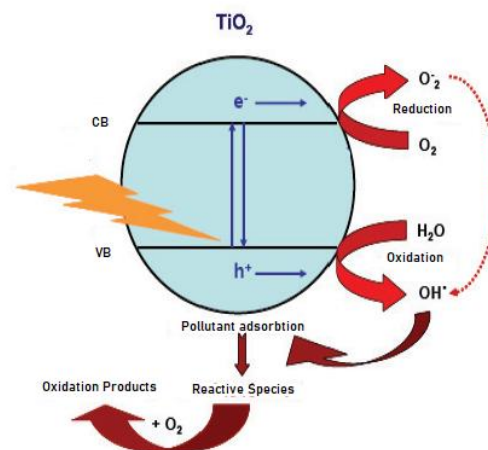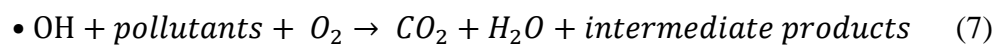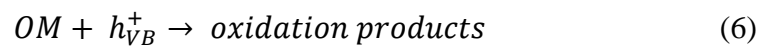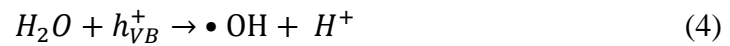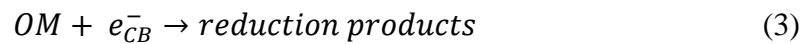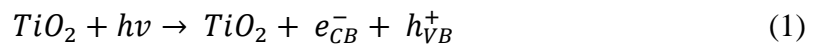
Figure 3. Mechanism of heterogenous photocatalysis, using TiO_2 as photocatalyst. Adapted from (Yasmina et al. 2014).

A molecule that shows up to be an advantage to photocatalytic reactions is oxygen. Indeed, some studies presented better results when oxygen is in the reaction medium, decreasing the concentration of the pollutant much faster than the reaction without O_2. This can occur because of the production of radicals •OH and the recombination of electron-hole pairs (Yasmina et al., 2014, Jiménez et al., 2015).

When the kinetics of the photocatalysis reaction for degradation of organics pollutants is considered, the model normally chosen is Langmuir-Hinsgelwood (Sraw et al., 2018; Zendehzaban et al., 2013; Abhang et al., 2011). As the reaction occurs, intermediates are formed, which can influence the reaction kinetics. Therefore, the Langmuir-Hinshelwood model can be expressed as a function of initial concentration, showed in Equation 8

$$-\frac{dC_0}{dt} = \frac{k\,K\,C}{1+KC} \qquad (8)$$

where C is the concentration of the pollutant (mg. L^{-1}), k is the reaction rate constant (min^{-1}), K is the equilibrium adsorption constant (L.mg^{-1}) and t is reaction time (min). Since the solution is diluted, the expression can be represented as a first order kinetic, Equation 9,

$$-\frac{dC}{dt} = k_{ap}\,C \qquad (9)$$

where k$_{ap}$ is the kinetic constant of a pseudo-first order reaction (min^{-1}) and t is the reaction time. Integrating this equation, with the initial condition $C_{(t=0)} = C_0$, the expression turns as Equation 10:

$$-\ln\frac{C}{C_0} = k_{ap}\,t \qquad (10)$$

2.2.2 TiO$_2$ Photocatalysis

The choice of TiO$_2$ as the semiconductor in this study is due to its good chemical and physical properties for photocatalysis. A semiconductor for the degradation of water pollutants should be inert, easy to use and produce, photocatalytically active, and be activated by radiation. This photocatalyst has all these characteristics, as well as its low-cost and high stability toward photo corrosion (Chirwa & Bamuza-Pemu, 2010; Danfá et al., 2021). Another property of TiO$_2$ is the capacity of working at ambient temperature and pressure, without adding other compounds, due to its band gap (3.2 eV). It is considered an obvious choice for photocatalytic processes (Yasmina et al., 2014).

TiO$_2$ has three distinct crystalline forms: anatase, rutile, and brookite, being the first two the most common phases (Yasmina et al., 2014). Anatase form has not only the most efficient photocatalytic activities but also the easiest form to produce (Chirwa & Bamuza-Pemu, 2010). Al-Taweel and Saud (2016) studied the synthesis of pure TiO$_2$ nanoparticles in anatase form with sol-gel method. Figure 4 shows the SEM image of these nanoparticles in this study (Al-Taweel & Saud, 2016).
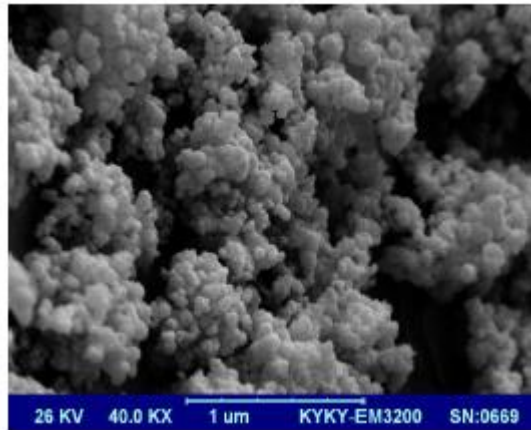
Figure 4. SEM image of TiO$_2$ nanoparticles. Adapted from (Al-Taweel and Saud 2016).

Several commercial forms of TiO$_2$ have been proven to be efficient, while P25 Degussa TiO$_2$ is the most used form. It is made of a non-porous ratio of 70:30 (anatase-rutile), with a specific surface area (BET) of 55 ± 15 m^2 g^{-1} (Yasmina et al., 2014).

2.2.3 TiO$_2$ supported in LECA

Although all the advantages that TiO$_2$ has as a powder, some drawbacks may also be indicated. In particular, due to its small dimensions (nanoparticles), when the powder is used in a photocatalytic reactor, it is difficult to do its separation and reutilization, increasing the operating cost (Danfá et al., 2021). To overcome this problem, ceramic supports may help in the recovery of the catalyst from the reaction solution (Danfá et al., 2021; Shavisi et al., 2014).

Comparing all the materials from which supports can be made, ceramic materials stand out, taking into account their physical and chemical properties. In particular, LECA is a ceramic material that is being widely used to immobilize TiO$_2$ powder (Danfá et al., 2021). Figure 5 shows the common appearance of LECA and its different commercial sizes (Rashad, 2018).

Figure 5. LECA with different sizes (Rashad 2018).

LECA is a resistant material with high porosity (73-88%) and low density. LECA particles often float on the surface of aqueous solutions, being easily exposed to UV light when the photocatalyst is immobilized on it (Al-Taweel & Saud, 2016). In Figure 6 it can be seen the interior of the LECA particle, where air cavities (pores) are presented, which is the reason why LECA is a material with low density and high porosity (Rashad, 2018).

Figure 6. Image inside of a LECA particle, where pores of different sizes can be seen (Rashad 2018).

Beyond the physical characteristics, the non-toxicity of the material, the low cost, and its high lifetime utility turns LECA a great possibility to use at an industrial scale (Zendehzaban et al., 2013). For all these reasons, LECA is the support used in this study. In a study made by Shavisi et al. (2014), LECA was used as a support to TiO_2 powder to degrade ammonia and in the study made by Zendehzaban et al (2013), TiO_2 was immobilized in LECA, being used in the treatment of ammonia via photocatalysis.

Figure 7 shows SEM images of LECA and TiO$_2$ in LECA (Zendehzaban et al., 2013).
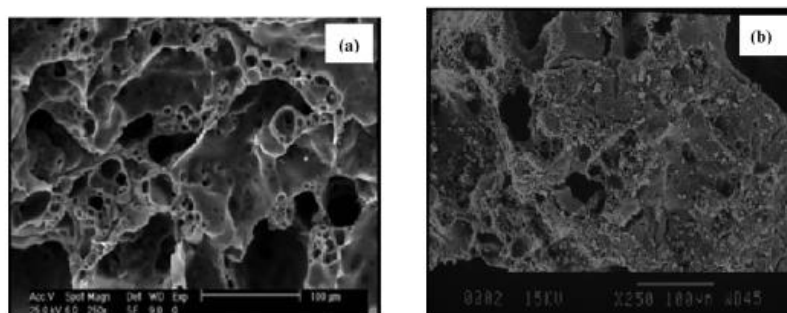
Figure 7. (a) SEM image of LECA. (b) SEM image of LECA with TiO$_2$ impregnated over it. Adapted from (Zendehzaban, et al 2013).

2.3   Reactor configuration

Reactor layout is an important part of heterogenous photocatalysis, to turn reactions as efficient as possible (Abhang et al., 2011). Several factors need to be evaluated not only technically, but also economically. The concentration of pollutants and catalysts, type of irradiation, and mass transfer of pollutants are some of the factors that need to be studied (McCullagh et al., 2011).

The main issues to scale-up these reactors are if the provision of the specific surface area of the catalyst is high enough and if the illumination across this area is uniform (McCullagh et al., 2011). To use photocatalytic reactors in industrial applications, it is necessary to optimize the layout and operating parameters, such as geometry, radiation type, type of catalyst, and concentration (Abhang et al., 2011). The geometry of the reactor is related to the type of radiation, to collect the most emitted radiation as possible (Bouchy & Zahraa, 2003).

For wastewater treatment, photocatalytic reactors are divided into two types of configurations that depend on how are the photocatalyst particles placed in the reactor: if the particles are suspended in the medium, or immobilized (Hossain, 2019). In this dissertation, a slurry reactor and a fixed bed reactor were studied.

2.3.1 Slurry reactor and fixed bed reactor

Slurry reactors utilize the catalyst particles suspended in an aqueous fluid (Inglezakis & Poulopoulos, 2006), allowing a fast reaction rate, as well as a larger surface area and lower mass transfer restrictions compared to fixed-bed reactors (Ren et al., 2021). This type of reactor can be designed with big dimensions (Bouchy & Zahraa, 2003). If agitation is adequate, the concentration of pollutants and catalyst is homogeneous in the volume of the reactor.

On the other hand, fixed-bed reactors, or packed-bed reactors can operate in continuous and batch modes (McCullagh et al., 2011), which the liquid solution flows through a tube. In this configuration, a tube is filled with a catalyst in particle form, and it is fixed in the reactor volume (Inglezakis & Poulopoulos, 2006). This configuration has the main advantage of using the catalyst in static conditions, and thus the erosion damage is minimized. These two reactor layouts can be observed in Figure 8.
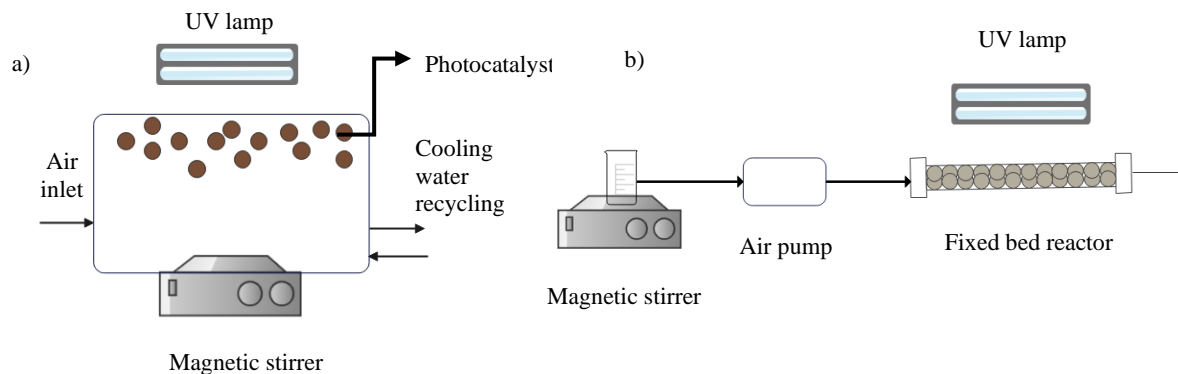
Figure 8. (a) Slurry type reactor (b) Fixed bed reactor Adapted from (Shavisi, et al. 2014; Sacco, Sannino, and Vaiano 2019)

3. State of Art

In this chapter, state of the art is described, where SMX effluent concentration is compared to human consumption in three different European countries. Secondly, several CECs are evaluated through different types of effluent, from freshwater to WTTPs. Furthermore, it is analyzed different reactor layouts, and these are compared regarding the type of radiation that is used, UV or solar.

3.1   SMX in effluents

Table 3 shows the consumption of SMX, mg per capita and day, in three European countries: Spain, Switzerland, and Sweden. Besides this information, it can be observed the wastewater discharged from European rivers, based on the water consumption in Europe. The predicted effluent concentration is based on the values that are expected.

Table 3. Consumption of SMX in some European countries, per mg cap^{-1} d^{-1}, as well as the wastewater discharges from rivers and their predicted and measured effluent concentration, in ng L^{-1} (Johnson et al. 2015).

Country	SMX consumption (mg cap^{-1} d^{-1})	Wastewater discharge (L cap^{-1}d^{-1})	Predicted effluent concentration of SMX (ng L^{-1})	Measured effluent concentration of SMX (ng L^{-1})
Spain	0.633	208	285	438
Switzerland	0.853	328	76	280
Sweden	0.440	205	65	70-233

Observing the SMX consumption in these three countries, it can be shown that the population in these regions consumes a great amount of this drug, which leads to the conclusion that, as it was mentioned previously, SMX is consumed at a high-level scale. This can be explained by the fact that SMX is used in several activities, from human to animal health. Furthermore, data in Table 3 demonstrate that SMX concentration measured is higher than was predicted, which can mean that the quantity of SMX consumed is partially excreted. This high release of SMX is a subject of concern since higher concentrations of this antibiotic can elevate bacterial resistance.

Table 4 shows different effluents and their SMX concentrations, from all around the world. There are several types of effluent evaluated, from seawater to WTTP. As it was mentioned earlier, since SMX is used on a large scale, it is common to appear in different types of effluent.

Table 4. Different types of effluent, SMX concentration in them and occurrence and percentage of removal with different methods.

Effluent type	Country	Concentration (ng L^{-1})	Occurrence (%)	Removal Efficiency (%)	Reference
Groundwater	Germany	410	-	-	(Sacher et al., 2001)
	USA	1110	23.4%	-	(Barnes et al., 2008)
	Spain	13.2	100%	-	(López-Serna et al., 2013)
Hospital effluent	Portugal	890	-	-	(Varela et al., 2014)
	Korea	2200	37.5%	-	(Sim et al., 2011)
Municipal wastewater	USA	920	100%	-	(Vidal-Dorsch et al., 2012)
	Korea	175	76.5%	-	(Sim et al., 2011)
River	Canada	1.9	64%	-	(Pulicharla et al., 2021)
	China	37	100%	-	(Xu et al., 2007)
	Bangladesh	1.39	70%	-	(A. Hossain et al., 2018)
Seawater	USA	0,05	70%	-	(Vidal-Dorsch et al., 2012)
	Italy	1.70	100%	-	(Brumovský et al., 2017)
WWTPs	USA	680 ±0.03	-	-	(Batt et al., 2007)
	Portugal	2200	92%	≈ 70%	(Gaffney et al., 2017)
	India	342	100%	≈ 40%	(Mohapatra et al., 2016)
	Australia	270	100%	25%	(Watkinson et al., 2007)
	Mexico	310	-	20%	(Brown et al., 2006)

From Table 4, it can be concluded that SMX was detected in several countries from all around the world, which confirms the high levels of consumption. The concentration values are from 0.05 to 2200 ng L^{-1} (Vidal-Dorsch et al., 2012; Sim et al., 2011; Gaffney et al. 2017). Observing with more detail river and seawater effluents, high values of SMX concentration are shown. This can indicate the inefficiency of WTTPs to treat this kind of effluent, leading to concentrations that affect the aquatic environment.

It can be shown that the occurrence of SMX has values between 23.4% to 100%, being this last value present at least in one example of each type of effluent (López-Serna et al., 2013; Vidal-Dorsch et al., 2012) (Xu et al., 2007; Brumovský et al., 2017; Watkinson et al., 2007). Thus, when the occurrence is 100%, it means that SMX appears in all the samples. According to Gaffney et al. (2017) from all the antibiotics that were detected in the samples, SMX was the one that had the highest occurrence value (92%) and it reached a higher concentration value of 5300 ng L^{-1} at the peak of winter, which can be concluded that exists a seasonal impact. This is expected, since winter is the season with more cases of respiratory diseases, and one of the uses of SMX is to treat these types of illnesses.

Removal efficiencies were also evaluated in Table 4. It can be observed that the efficiencies are from 20% to approximately 70% (Brown et al., 2006; Gaffney et al., 2017). The treatments used in conventional WTTPs are not enough to achieve the complete degradation of SMX, which leads to the discharge and, consequently, the contamination of rivers and other natural water bodies.

3.2 Reactor layout influence in photocatalytic oxidation processes

The study of reactor layout has several aspects to be considered to reach optimal degradation values. Radiation type, the photocatalyst dosage, the contact type, and different recirculation flowrates were assessed for slurry and fixed bed reactors. Experiences with UV and solar radiation were analyzed to observe the effects of these parameters in the reactor design.

3.2.1 UV radiation

A photocatalysis reaction, as like said previously, occurs with the use of a semiconductor and with radiation. In this section, several effects are evaluated, such as catalyst dosage and recirculation rate, using the same radiation, UV.

Table 5 summarizes different experiments where it can be seen different reactor layouts. All these experiences were conducted with UV lamps, and there were used different photocatalytic supports for the degradation of several CEC.

Table 5. Different experiences using UV-lamps with different reactor designs and their results.

Type of catalyst	Type of reactor	Reactor geometry	Solution volume (L)	Experiment	Operating conditions	Results	Reference
TiO$_2$ (P25)/perlite	Slurry	Pyrex glass vessel	1.5	Degradation of ammonia in wastewater	UV-C (125 W) (λ = 254 nm), 11.70 g L^{-1} of catalyst, 170 mg L^{-1} of ammonia, T = 20ºC, mixing	• The optimum pH is 11 • At the optimum pH, 64.3% of ammonia was removed • Increasing the capacity of the lamp (from 125 W to 250 W) the removal efficiency increases to 80% • Efficiency removal reaches 68.0% at 180 min with optimum operating conditions • k = 0.888 mg (L min)$^{-1}$	(Shavisi, et al., 2014a)
TiO$_2$/GAC	Slurry	Cylindrical batch reactor	2.0	Photocatalytic oxidation of sulfadiazine (SDZ)	UV-C (14 W) (λ= 254 nm), 1-6 g L^{-1} of catalyst, magnetic stirrer	• k = 0.09 min^{-1} • TOC improved by 61% when GAC support was used • Total removal of SDZ after 60 min at the optimum operation conditions (5 g L^{-1} and 28 W)	(Yadav et al., 2018)
TiO$_2$(P25)/TGS	Fixed bed	Cylindrical column	0.250	Photocatalytic degradation of paracetamol	Solar radiation sodium vapour (400 W) (λ = 244 nm), 50 cm distant from the column, 50 mg L^{-1}, T = 20ºC, 0.5 g L^{-1} of catalyst, air flow rate of 0.8 mL s^{-1}	• 42% of paracetamol degradation within 8 h of irradiation • Paracetamol removal reaches high values after 4 h of irradiation	(Borges et al., 2015)
TiO$_2$(P25)/clay beads	Fixed bed	Cylindrical column	1.0	Degradation of pesticide monocrotophos (MCP) polluted water	UV (20 W) (λ= 365 nm), T = 25±1 ºC, pH = 5, 25 mg L^{-1} of MCP, mass of photocatalyst support = 1121.7 g with 12.46 mm of diameter and 26.68 g of TiO$_2$, flowrate = 400 mL min^{-1}	• Efficiency of 79% of degradation of MCP after 30 cycles • k = 5.35 × 10^{-3} min^{-1}	(Sraw et al., 2018)

Shavisi, et al. (2014) studied the degradation of ammonia, where several aspects were analyzed. One of the factors was the light intensity at the suitable wavelength radiation, where electron-hole formation in photochemical reactions is directly dependent on the intensity of light. These authors used three lamps with different powers and concluded that the photocatalysis reaction rate increased as power rise, due to more catalyst activation.

Yadav et al. (2018) proved that the increase in the catalyst amount improves sulfadiazine (SDZ) degradation. This can be explained by the absorption of more photons into TiO_2 particles, which leads to the higher production of reactive species. However, when the degradation profiles of SDZ were observed for higher catalyst loads, it was noticed that the percentages of degradation were very much alike. This can indicate that a high catalyst load does not increase the removal efficiency. This is mainly because of the turbidity created in the solution and the agglomeration of TiO_2 particles, which caused scattering and blocking of the UV light. Although the system with TiO_2 without support showed to be effective for the SDZ degradation, the fact the particles of the catalyst penetrate the solution can cause environmental problems (Yadav et al. 2018). This turns out to be an advantage of using a supported catalyst, as previously mentioned.

In the study conducted by Borges et al (2015), paracetamol was degraded through a fixed-bed reactor. The authors concluded that with a lower flowrate, 0.8 mL s^{-1}, the efficiency of removal reached an optimal value of about 42%. Compared to the previous studies, this degradation value is significantly lower, since radiation couldn't reach all the particles of photocatalyst in the reactor (Sacco et al., 2019).

Sraw et al. 2018 studied different recirculation flowrates in a fixed-bed reactor. The recirculation rates studied were 100, 200, 400, 600, and 800 mL min^{-1}, throughout 5 h. When the flowrates were from 100 to 400 mL min^{-1}, the pesticide MCP had low degradation efficiencies, from 57.79% to 78.57%. When low recirculation rates were tested, it may not allow the optimum contact between the catalyst and MCP molecules, which lead to lower degradability. On the other hand, when the flowrate raised to 400 mL min^{-1}, more MCP molecules came across the TiO_2 particles' surface, which lead to more hydroxyl radicals (•OH) and, for this reason, lead to more degradation. However, when the flowrate increased to 800 mL min^{-1}, it was observed a decrease in the degradation rate (66.23%). This can be explained by the fact that MCP molecules had a lower contact time with TiO_2 particles, resulting in a smaller degradation efficiency. In this case, 400 mL min^{-1} was considered the optimum value, to obtain a steady residence time and to maintain the catalyst in the support by having a laminar flow.

3.2.2 Solar radiation

Just like the studies using UV radiation, it was also compared different effects under solar radiation. Some of the parameters evaluated were radiation and different flowrates.

The studies about solar radiation are mentioned in Table 6. Since solar radiation is a free and endless resource, it can be economically advantageous in comparison to UV-A radiation with lamps. Moreover, the solar spectrum contains a fraction of UV-A, and due to this can be a suitable option to replace UV-A lamps.

Table 6. Different experiences using solar radiation with different reactor designs and their results.

Catalyst	Type of reactor	Reactor geometry	Solution volume (L)	Experiment	Operating conditions	Results	Reference
TiO$_2$/LECA	Slurry	Cylindrical vessel	5	Degradation of ammonia in petrochemical wastewater	Solar radiation (09:00– 16:00 h, 125 g of catalyst in the solution, concentration of 975 ppm of ammonia), air pump (10 L min^{-1}), and another reactor with a magnetic stirrer	• Optimal efficiency in three days was 96.5% with pH=11 and dosage of catalyst = 25 g L^{-1}, both aeration methods had similar results regarding the degradation of ammonia • k = 2.063 mg (L min)$^{-1}$	(Shavisi, , et al., 2014b)
TiO$_2$/pebbles	Fixed bed	Rectangular fixed bed reactor	0.66	Decolorization of reactive dye solutions of textile wastewater	Solar radiation (10:00h –15:00h), 0.79 g of catalyst, inclined reactor, Batch l = 10-fold, and Batch ll = 5-fold (dilution with a factor of 10 and 5), air flow	• k = 2.479 x 10^{-2} – 7.858 x 10^{-2} min^{-1} • the most efficient operation conditions were: pH = 8.3, flowrate = 0.138 g L^{-1}, 25 mg L^{-1} of catalyst • color reduction of 72% (Batch l) and 54% (Batch ll), TOC = 3-35%	(Rao et al., 2012)
Fe-TiO$_2$/clay beads	Fixed bed	Flat Plate Photocatalytic Reactor (FPPR)	0.50	Degradation of carbendazim (CBZ) in water	Solar radiation (10:00h-16:00h), 8 kg m^{-3} of CBZ, pH = 6.3, 4 g of catalyst for 50 beads, sun intensity = 600 W m^{-2}, air flow	• 93% of CBZ degradation after 300 min of reaction • k = 0.15214 kg m^{-2} min^{-1} • With only TiO$_2$, efficiency of degradation is 82% and k = 0.1311 kg m^{-2} min^{-1}	(Kaur et al., 2018)

Shavisi et al. (2014) used two different batch reactors, one with aeration and the other with a magnetic stirrer system. The degradation efficiency of ammonia in these two reactors was very similar, which can be explained by the adsorption of N_2 molecules into the particles of TiO_2/LECA. When solar and UV radiation was compared, UV radiation presented a higher value of degradation than solar radiation. According to the authors, this can be explained due to the position of the photocatalyst on the surface of the effluent, whereas in the case of UV it was more efficient. This effect lead to more activation of TiO_2 under UV light rather than solar, which lead to a higher degradation efficiency.

In the study conducted by Rao et al (2012), the recirculation flowrate was a parameter studied, where the flow had a laminar regime. Increasing the flow rate from 0.138 L min^{-1} to 0.195 L min^{-1}, lead to a decrease in degradation value. This was a contradicting conclusion since with an increase in the flow rate, the fluid residence time decreases and the number of passes per unit time increases, leading to an increase in the efficiency of degradation. These results can be explained by the fact that the reactor had not an ideal flow behavior. With the reactor in a horizontal position, the catalyst was submerged in the liquid and when the flow rate increased, a major fluid by-passing could occur, which lead to lower degradation values.

Lastly, Kaur et al. 2018 also studied the effect of the recirculation flow rate on the degradation values. When lower flow rate values were tested, contact time is higher, but it increases the time necessary to have an effective degradation value. Contrary results are shown when high recirculation rates are implemented, leading to a shorter contact time and, consequently, lower values of photocatalytic degradation. The authors concluded that a certain recirculation rate (100 x 10^{-6} m^3 min^{-1}), allows a higher residence time and avoids turbulence, which can cause the removal of the photocatalyst of the support used, favors

3.3   Photocatalyst reuse

Another important aspect is the recyclability of the photocatalyst. One of the reasons to have the photocatalyst in a support is to have the capacity to reuse it while the degradation values maintain high enough. Some aspects must be taken into account to evaluate the efficiency of the reuse such as the number of cycles, the reaction time, what type of treatment the photocatalyst suffered to be supported, and the different reactors' layouts. These examples can also show if the photocatalyst can operate in continuous mode during high periods of time. Table 7 shows examples where all these effects are compared with each other.

Table 7. Photocatalyst reuse experiences, the reactor design, and the reaction conditions and their results.

Catalyst	Number of cycles	Experiment	Degradation efficiency and reaction time (min)	Reactor layout	Reaction Conditions	Results	Reference
TiO$_2$/Ceramic material	3	Degradation of methylene blue	65% (60 min)	Slurry	Continuous reuse of photocatalyst UV-C lamp (λ= 254 nm) 5 mg L^{-1} of methylene blue	- Three samples were tested. - In the first one, 24% of photocatalytic activity was lost in the second cycle and 45% in the third sample. - In the third sample, although it presented less degradation efficiency, it maintained a high value of photocatalytic activity, that can be explained by the heterogeneity of the ceramic support and the saturation of by-products produce during the reaction.	(Peters et al., 2018)
TiO$_2$/glass beads	3	Degradation of ammonia in petrochemical wastewater	96.5% (420 min)	Slurry	Solar radiation (09:00h – 16:00h), pH=11, dosage of catalyst = 25 g L^{-1}, 125g of catalyst in the solution, concentration of 975 ppm of ammonia	- The efficiency decreased about 14% each time the photocatalyst was reused. - Before the reuse step, the photocatalyst suffer a four-stage regeneration process.	(Shavisi, et al., 2014b)
TiO$_2$/ clay beads	30	Degradation of MCP	78.57% (420 min)	Fixed Bed	UV (20W) (λ= 365nm), pH = 5, 25mg L^{-1} of MCP, flowrate = 400 mL min^{-1}	- Continuous cycles were made during the whole reaction, using the photocatalyst without any drying step. - Since the first to the last cycle, the degradation efficiency maintains high values (78.57% to 70.11%).	(Sraw et al., 2018)
TiO$_2$/ clay beads	40	Degradation of carbendazim	87% (300 min)	Fixed Bed	Solar radiation (10:00h-16:00h), 8 kg m^{-3} of CBZ, pH = 6.3, 4 g of catalyst for 50 beads, sun intensity = 600 W m^{-2}	- The 40 cycles were continuous and conducted for 5 hours - In the last cycle, the degradation efficiency reached approximately 66%. - When TiO$_2$ was dopped with Fe, it had better results, from 93% of degradation in the beginning to 87% in the 40th cycle.	(Kaur et al., 2018)

In the study conducted by Peters et al. (2018), it was noticed that the three samples tested presented similar values for the degradation of methylene blue. The first sample had the highest degradation values but was the one that lost the most photocatalytic activity in the third use (45%). The third sample had better efficiency values, reaching 15% of photocatalytic activity loss in the third use. This happened because this sample had the most quantity of TiO_2 impregnated in the support, which lead to better values. Another explanation is the fact that the reaction produced by-products, which did not desorb from the surface of the photocatalyst.

Shavisi, et al. (2014b) before reusing the photocatalyst made a regeneration process to remove adsorbed ammonia from the photocatalyst surface. This process consisted of washing, putting the photocatalyst in a mixing system, then in a sodium chloride solution and, lastly, it was treated at high temperatures. This removal can prevent loss in degradation efficiency. The degradation efficiency decreased by approximately 14% in each cycle. This can be explained by the fact that as the photocatalyst is being used, the adsorption capacity and its activation sites decrease, which lead to lower degradation rates per cycle.

In the studies of Kaur et al. 2018 and Sraw et al. 2018, both photocatalyst reuses were done in several continuous cycles. Both reuse reactions showed a small difference between the first and the last cycle. This can be explained by the absence of photocatalyst washing and drying processes before the reuse, which means that the continuous process is more efficient.

4. Materials and Methods

4.1 Materials

- **LECA**

The LECA used in this study was obtained from LECA Portugal S.A. and was type S (according to the particle size). The sample received in the laboratory had diameters between 1-5 mm. This sample was then sieved to a range of 3.36-4.76 mm. The procedure of LECA preparation to be used in immobilization technology was made according to a previous work (Oliveira, 2021). Before its usage, LECA was washed with water, dried at 105 ºC, and stored in the lab for later use. The particles used in this study are represented in Figure 9.

Figure 9. LECA of type S used in this study.

- **Titanium Dioxide**

Titanium Dioxide (TiO_2) used in this study was *Aeroxide P25* (70% anatase and 30% rutile) and was purchased from Acros Organics, with a purity of $\leq 99,5\%$. Its physical and chemical properties are showed in Table 8 (Pubchem, 2022b).

Table 8. Chemical and physical properties of TiO_2.

Chemical Formula	TiO_2
Water solubility (mg cm^{-3})	> 1
Density (g cm^{-3})	3,9-4,3
Molecular weight (g mol^{-1})	79,866
Particle size (nm)	± 10
Specific surface area (m^2 g^{-1})	35-65

- **SMX**

To prepare the synthetic effluent for this study, sulfamethaxazole (SMX) with a purity of 98% was purchased at Alfa Aesar. A stock solution was made with a 20 mg L^{-1} concentration, and to dissolve the powder in ultrapure water, it was used an ultrasound bath (J.P. SELECTA, Ultrassons MEDI-II, 40Hz). After all these processes, the stock solution was diluted to obtain an initial concentration of 1 mg L^{-1} that was used in all the assays.

4.2   Photocatalyst preparation

The impregnation of TiO_2 in LECA followed a procedure developed in a previous work (Oliveira, 2021). The steps are detailed in Annex I. The TiO_2 suspension loads selected are 3.6 and 5% (w/w), based on the same work, and thus, the tested catalysts are hereafter referred to as 3.6%TiO_2/LECA and 5%TiO_2/LECA.

4.3   Experimental procedures to evaluate reactor layout

4.3.1 Slurry reactor
4.3.1.1   UV-A radiation

The assays for heterogenous photocatalysis with UV-A radiation were made using a glass reactor of 150 mL, while the working volume was 100 mL of synthetic effluent. The radiation was provided by a Mineralight lamp Model UV GL-58, with maximum peak emission at 366 nm. An air pump AC-9601 with a flowrate of 1.8 L min^{-1} was used during the reaction. To avoid external radiation and to maintain the lamp radiation in the system as much as possible, a box filled with aluminum foil was used to involve and cover the reactor.

The reaction had a duration of 120 min, where the samples were taken at the beginning of the reaction, after 60 min, and at 120 min. All the samples were filtered through a 0.45 µm cellulose acetate filter. Three different photocatalyst concentrations were used in the assays: 5 g L $^{-1}$, 15 g L $^{-1,}$ and 25 g L $^{-1}$. When the reaction was complete, the photocatalyst was collected and dried in an oven for 12 h at 105 ºC. When dried until constant mass, the catalyst was weighted to analyze the mass loss during the reaction. To control the pH of the solution, a pH measurer (Crison micropH 2002) was used. Figure 10 (a)-(b) shows a schematic representation of the system used. Figure 10 (a) depicts the reactor agitated with air and Figure 10 (b) shows the system with magnetic agitation at 60 rpm.
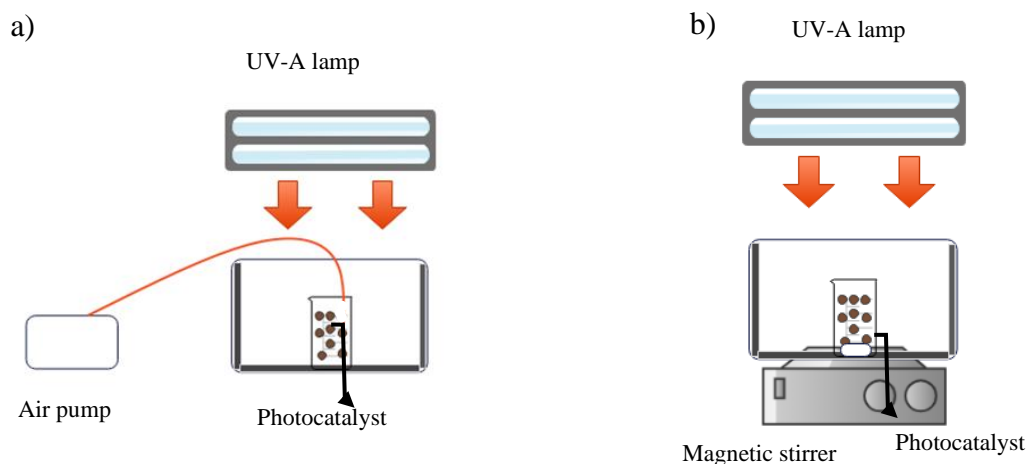
Figure 10. a) Slurry reactor (150 mL) with an UV-A lamp and different mixing types with an air pump b) a magnetic stirrer.

4.3.1.2 Solar radiation

All the photocatalytic experiments under solar radiation were made with a 150 mL glass reactor at the same conditions of UV-A radiation as well as the experimental procedure regarding tested concentrations, liquid sample collection, and photocatalyst recovery. Figure 11 shows a schematic representation of the system used under solar radiation.
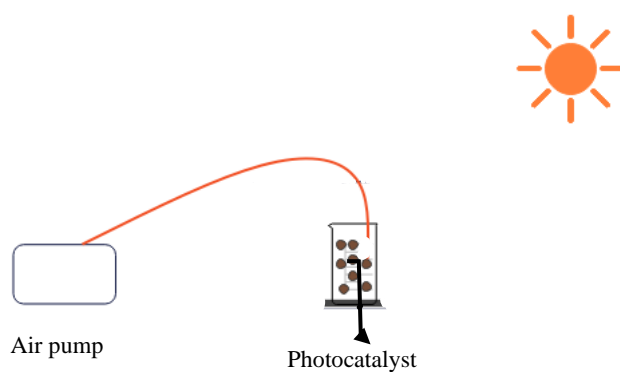
Figure 11. Slurry reactor (150 mL) under solar radiation, using an air pump.

4.3.2 Fixed bed reactor

4.3.2.1   UV-A radiation

The fixed-bed experiments using UV-A radiation were conducted using a tubular reactor with 100 mL of working volume, with a laminar regime, established in Annex II, and a recirculation feed of 0.012 L min^{-1} using a pump (Minipuls 3). The photocatalyst was set in a column with 10 mm x 330 mm and placed in a vertical position. The UV-A lamp used was a Mineralight Lamp Model UVGL-58 with a maximum peak emission of 365 nm. The reaction had a duration of 120 min. Liquid samples were taken at the beginning, after 60 min, and at 120 min. The photocatalyst concentration in the column was 25 g L^{-1}, where L is in volume of solution to be treated, and glass spheres filled the column. The diameter of the glass spheres was 5.8×10^{-3} m and bed porosity (ε_v) was approximately 0.50. Figure 12 shows a schematic representation of the experimental setup used, where it can be seen that the reactor is placed inside a box covered with aluminum foil.
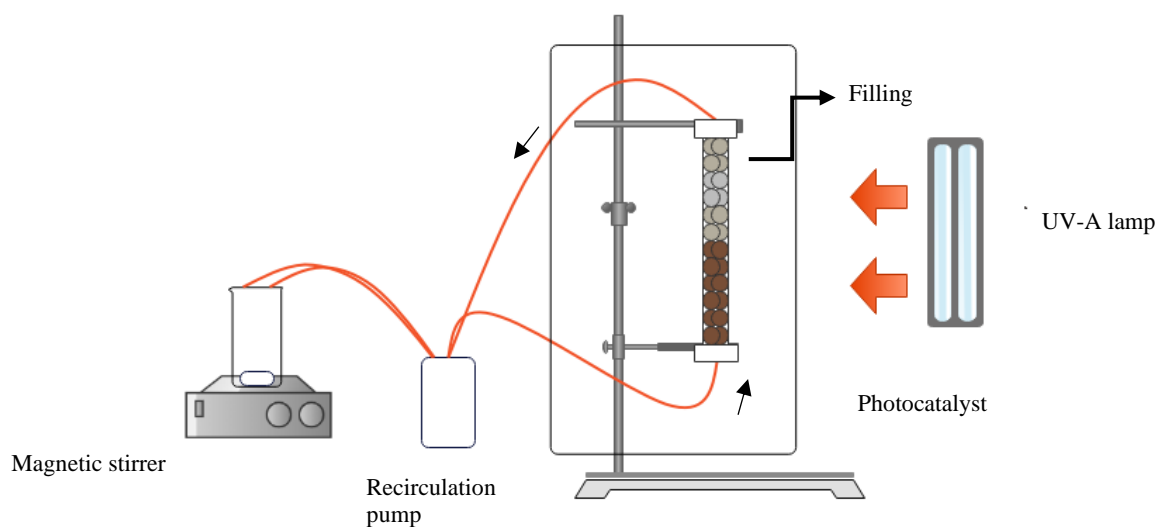
Figure 12. Fixed bed reactor under UV-A radiation.

4.3.2.2   Solar radiation

The assays made with solar radiation were conducted similarly to the ones made with UV-A radiation inside the lab. The flowrate was a parameter studied, so it was used a flowrate of 0.006 L min^{-1} and 0.012 L min^{-1}, where the regime for both recirculation feeds was established in Annex II. In these assays, the reaction time was 180 min, where samples were taken before the reaction started and every 60 min. There were three types of photocatalyst distributions inside the column, as well as the column full of particles. These distributions are when the column is full, therefore 50 g L^{-1} of photocatalyst concentration, and the other three are when the column supports half of this value, thus 25 g L^{-1}, but with different distributions. All four distributions are shown in Figure 13, where it can also be seen the fluid direction through the column. Just like the UV-A radiation assays, the remaining space in the column was filled with glass spheres with the same dimensions. The ε_v was considered equal for all the distributions, with a value of 0.50. Figure 14 shows how the assays were conducted under sun radiation.
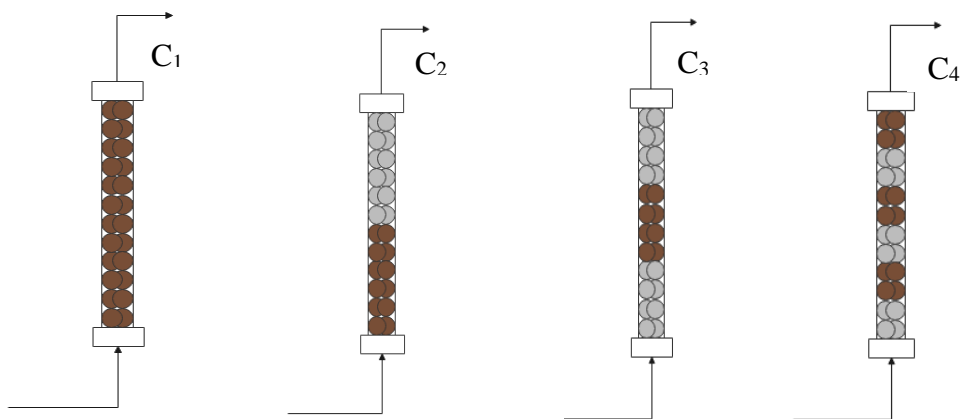
Figure 13. Four configurations used in the solar radiation assays: C_1 is with all the particles (50 g L^{-1}), C_2 is with half of particles (25 g L^{-1}) in the beginning of the column and filling upper it, C_3 is with half of the particles between the filling and C_4 is with half of the particles but with alternate layers of particles and filling.
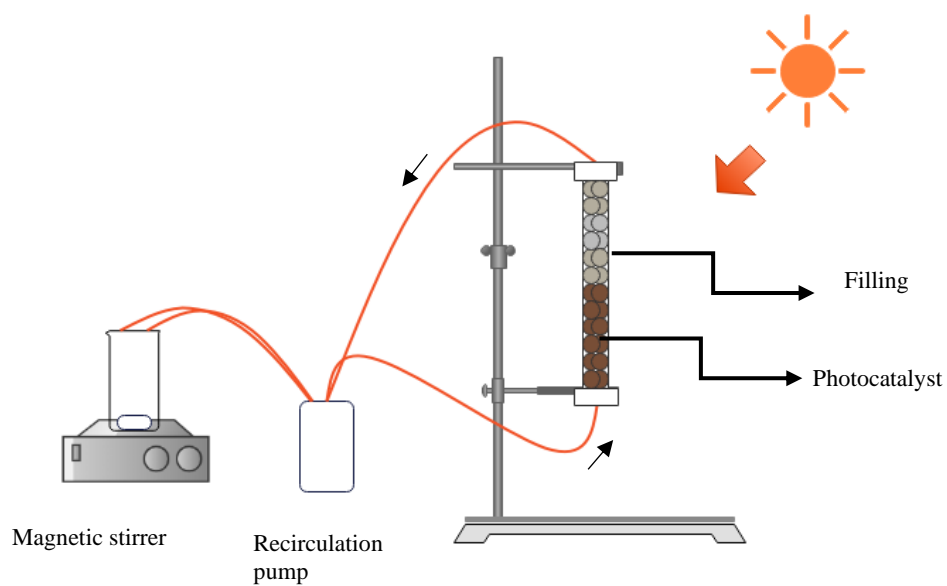
Figure 14. Fixed bed reactor under solar radiation.

4.4 Photocatalyst reuse

Photocatalyst reuse was also studied in this dissertation. This analysis was performed in two moments: when the effect of the mixing system was evaluated for the slurry reactor with 150 mL, and for the fixed bed distribution where the column had a concentration of 50 g L^{-1} which corresponds to the all column filled with photocatalyst (C_1). Before its reuse, and at the end of 120 min of reaction, the photocatalyst in the slurry reactor was dried at 105 ºC for 12 h. In the slurry reactor (150 mL), the photocatalyst was reused 2 times, while for the fixed bed reactor, it was reused 3 times.

4.5 Determination of SMX concentration

The concentration of SMX during the reactions was determined by high-performance liquid chromatography (HPLC). The equipment used was a Beckman-System Gold, where 100 µL of the sample were injected into a mobile phase made of 45% of methanol and 55% of acidic water (0.1% of ortophosphoric acid) with a 0.75 mL min^{-1} flowrate. The column used was C18 (SiliaChrom) at a constant temperature of 40 ºC and SMX was detected in a wavelength of 280 nm. The by-products analyzed, AMI and BZQ, were detected in a wavelength of 240 nm and the retention time was 5.3 and 6.2 min, respectively.

5. Results and Discussion

In this chapter, the results obtained during the assays were shown and discussed. The chapter is divided into three main parts: the effect of photocatalyst dosage, the effect of the reactor design, and the photocatalyst reuse.

5.1 Effect of photocatalyst dosage

In this section, the effect of different photocatalyst dosages on the SMX degradation rate was tested. This parameter is only analyzed for one configuration (slurry reactor), where UV-A radiation with aeration were used with the $3.6\%TiO_2/LECA$ and $5\%TiO_2/LECA$ photocatalysts.

5.1.1 Slurry reactor

The degradation rates for the three concentrations using UV-A radiation and aeration are demonstrated in Figure 15, tested for $3.6\%TiO_2/LECA$ and $5\%TiO_2/LECA$, and the mass loss during the reaction for the three concentrations. These degradation values are compared to the photolysis degradation value determined in a previous work of 15.8% (Oliveira (2021)).

a)   b)
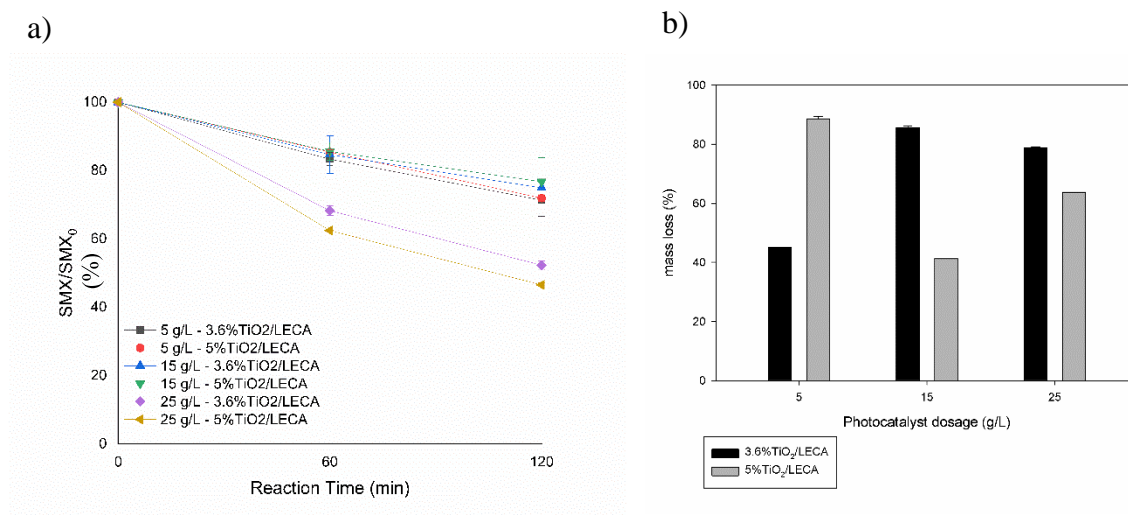
Figure 15. (a) SMX degradation rates for the different dosages of photocatalyst for $3.6\%TiO_2/LECA$ and $5\%TiO_2/LECA$ using UV-A radiation and aeration. (b) mass loss during the reactions.

Figure 15 shows that all the values using the photocatalyst are better than the photolysis, which proves the effectiveness of photocatalysis using TiO_2 supported in LECA.

When a higher concentration of photocatalyst is used, less SMX concentration is present at the end of the reaction. With catalyst at concentrations of 5 g L^{-1} and 15 g L^{-1}, the results are very similar for both 3.6%TiO_2/LECA and 5%TiO_2/LECA, while the concentration of 25 g L^{-1} stands out, with 47.7% and 53.5% of degradation after 120 min for 3.6%TiO_2/LECA and 5%TiO_2/LECA, respectively. These results occurs due to the presence of more photocatalyst in the system, creating a larger area for photons absorption by the photocatalyst particles, producing more reactive species, compared to lower photocatalyst concentrations (Yadav et al., 2018). Observing these results, the higher photocatalyst dosage is the ideal concentration to promote the degradation of this antibiotic. In the study of Shavisi et al (2014a), where the catalyst was supported in perlite, the efficiency of ammonia removal reached 68% at the end of 180 min.

In terms of TiO_2 loss, the three dosages had different results, due to the heterogeneity of the support. Being a porous material, LECA could have different quantities of TiO_2 nanoparticles impregnated in it, leading to different loss results.

5.2   Reactor layout effect in the reaction

After choosing the most efficient photocatalyst dosage, 25 g L^{-1}, other effects in the reaction were analyzed. These effects are related to the reactor layout: the effect of mixing type, and radiation. All these parameters were studied for the two different configurations, slurry reactor and fixed bed reactor.

5.2.1 Slurry reactor

5.2.1.1   Effect of mixing system

The two systems used to study the mixing conditions were aeration and a magnetic stirrer. The studies were conducted using 3.6%TiO$_2$/LECA and 5%TiO$_2$/LECA and the photocatalyst dosage selected from the previous section, 25 g L^{-1}, and a UV-A lamp. Figure 16 shows the degradation rates for both experiments and the mass loss that occurred during the reactions.
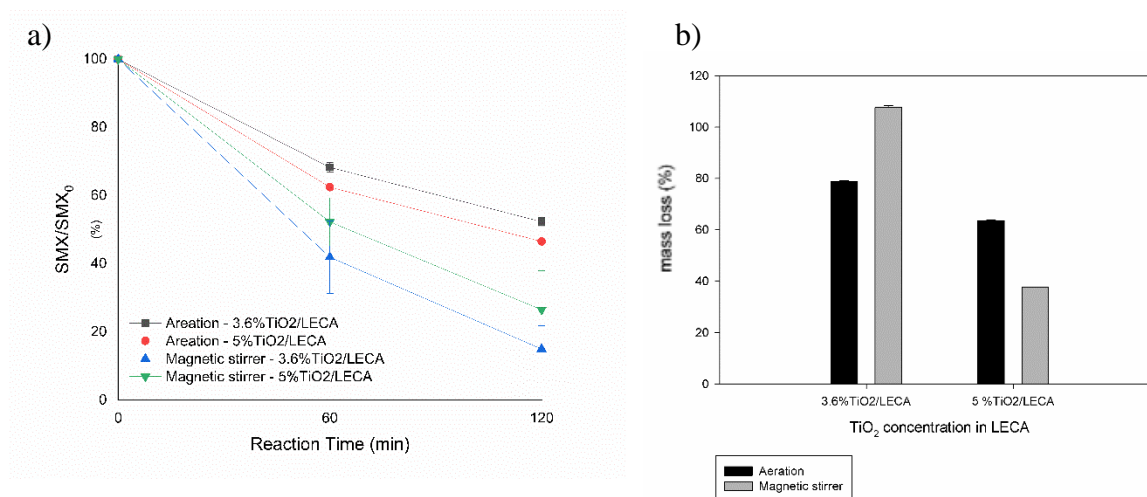
Figure 16. a) SMX degradation rates for the different mixing types of photocatalyst for 3.6%TiO$_2$/LECA and 5%TiO$_2$/LECA using UV-A radiation. (b) mass loss during the reactions.

According to Figure 16 a), the magnetic stirrer is the mixing system where SMX degradation values are higher, compared to aeration. This conclusion is valid for both photocatalysts (3.6%TiO$_2$/LECA and 5%TiO$_2$/LECA). However, in other studies such as Shavisi et al (2014a) the conclusion was that these two mixing systems had very similar SMX concentrations at the end of the reaction. Comparing the influence of the two TiO$_2$

concentrations in the catalyst, 3.6% TiO$_2$/LECA degraded the most, using the magnetic stirrer for mixing the solution.

Regarding the TiO$_2$ loss in Figure 16 b), it can be seen that when the magnetic stirrer was used for 3.6%TiO$_2$/LECA, the percentage of TiO$_2$ release is up to 100%. This result means that all photocatalysts impregnated in the support is lost, which can explain the high SMX degradation value in this experience. In fact, when TiO$_2$ is used as a powder, the efficiency of removal is higher than when in the support (Danfá et al., 2021). However, for 5%TiO$_2$/LECA, when the aeration is used, more TiO$_2$ is lost, but, when it comes to the magnetic stirrer, the results are the opposite. This can be related with better immobilization of TiO$_2$ when the 5% TiO$_2$/LECA suspension was used, which retained more when submitted to a stronger interaction. Moreover, to understand these values, a reuse of the photocatalyst in these two situations was made.

Figure 17 compares the degradation rates for both cycles and the mass loss in the second cycle for the two reactions using the aeration and the magnetic stirrer, for both 3.6%TiO$_2$/LECA and 5%TiO$_2$/LECA photocatalyst. Between the reaction periods, the photocatalyst was dried at 105 ℃ for 12 h.
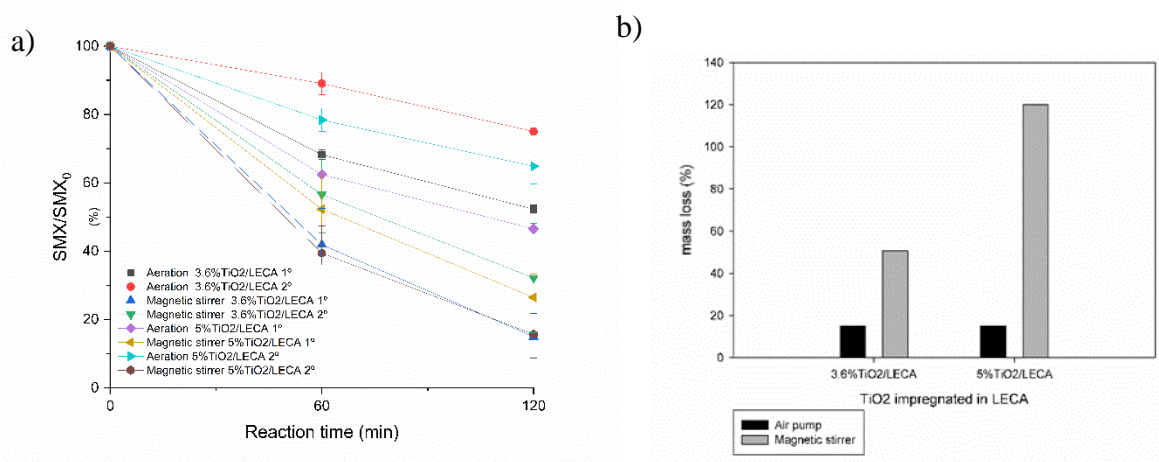
Figure 17. a) SMX degradation rates for the reuse of photocatalysts in the assays using different mixing types of photocatalysts for 3.6%TiO$_2$/LECA and 5%TiO$_2$/LECA with UV-A radiation. (b) TiO$_2$ loss during the reactions.

The analysis of the data in Figure 17 a), in a general view, it is possible to conclude that the photocatalytic activity decreased in the second cycle. For the 3.6%TiO$_2$/LECA, when the aeration was used, the efficiency was reduced to 22.7% and with the magnetic stirrer was reduced to 18.4%. But, when the 5%TiO$_2$/LECA photocatalyst was used, the efficiency between cycles in aeration decreased by 22.9%, while when the magnetic stirrer was used, the photocatalytic activity increased by 10.8%. Analyzing the mass loss, in the case of

3.6%TiO$_2$/LECA, the values are significantly lower compared to the 1st cycle, indicating that the most quantity of TiO$_2$ was lost in the first reaction. This agrees with the reduction in the SMX degradation efficiency at the second reaction. However, when confronting the values for the reaction using 5% TiO2/LECA and a magnetic stirrer, it lost the higher percentage of TiO$_2$. This can be explained to the liberation of TiO$_2$ from the support, leading to a higher degradation of SMX in this experience. It is important to mention the LECA loss during the magnetic stirrer experiments that can promote a higher release of TiO$_2$ particles to the solution.

5.2.1.2   Effect of the radiation

To compare the radiation type, studies under the sunlight were made for the slurry reactor. These reactions were performed in the Department of Chemical Engineering of the University of Coimbra and lasted 120 min. All the details regarding the solar radiation reactions are shown in Table 9.

Table 9. Information about the solar radiation observed during the experiments in June, 2022.

Photocatalyst concentration (w/w)	Date	Time	Solar Radiation Intensity (max-min) (W m^{-2})	Energy for 2 h (kJ m^{-2})
3.6%TiO$_2$/LECA	June 9th	1:30-3:30 PM	911-775	6455.7
5%TiO$_2$/LECA	June 28th	3:02-5:02 PM	868-622	5689.5

Figure 18 shows the values of SMX degradation for 3.6%TiO$_2$/LECA and 5%TiO$_2$/LECA, comparing UV-A and solar radiation in both scenarios, using aeration, and the mass loss at the end of the reactions.
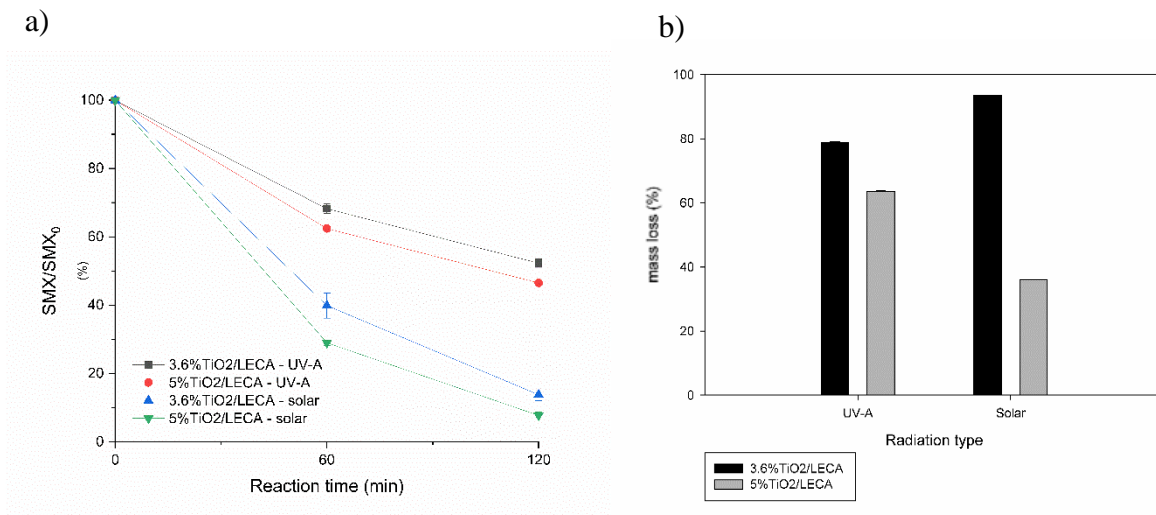
Figure 18. (a) SMX degradation rates for the two radiation types (solar and UV-A) using photocatalyst 3.6%TiO$_2$/LECA and 5%TiO$_2$/LECA and aeration; (b) mass loss during the reactions.

Firstly, to conclude about the photocatalyst efficiency under solar radiation, the values were compared with the degradation value under photolysis, using the same SMX concentration in the synthetic effluent and the same reactor configuration. This percentage was taken from previous work and the removal was about 17.5% after 120 min (Oliveira (2021)). Therefore, it can be concluded that photocatalysis lead to significantly higher degradation values. Indeed, from the results in Figure 18 a), it can be observed that solar radiation had a greater effect on the degradation of SMX, 86.2% and 92.3% for 3.6%TiO$_2$/LECA and 5%TiO$_2$/LECA, respectively. This is explained due the UV-A and UV-B radiation that are part of the 5% of the sun's radiation, as well as the photon flux intensity that was higher for solar radiation (Danfá et al., 2021; Ferreira et al., 2021). This radiation promotes better photocatalytic results, compared to a UV-A lamp. Comparing the two photocatalysts, it can be concluded that when 5%TiO$_2$/LECA is used, better results were obtained with solar radiation and with UV-A radiation. This photocatalyst has more TiO$_2$ impregnated in LECA, which lead to more photon's absorption at the photocatalyst surface, leading to a more effective degradation of SMX at the end of the reaction period. Regarding the values of TiO$_2$ loss for the solar reactions, 3.6%TiO$_2$/LECA had a higher percentage of mass loss. This can be explained because of the heterogeneity of the support, which can lead to higher or lower TiO$_2$ release into the reactional medium.

In order to compare the performance of UV-A and solar radiation reaction, it was determined the pseudo-first-order kinetic constant, for both radiations and by using the photocatalysts 3.6%TiO$_2$/LECA and 5%TiO$_2$/LECA. Table 10 summarizes the kinetic constants obtained in each case.

Table 10. Pseudo-first order kinetic constants of the reactions and their R square.

Photocatalyst	k_{ap} (min^{-1}) (R^2)	
	UV-A radiation	Solar radiation
3.6%TiO$_2$/LECA	0.00561 (0.9913)	0.01577 (0.9993)
5%TiO$_2$/LECA	0.00676 (0.9867)	0.0208 (0.9999)

As can be seen in Table 10, the R^2 is very close to 1 for all the kinetic constants, which means that the pseudo-first-order kinetic describe well the experimental data. Comparing the UV-A and solar radiation, the kinetic constants were higher for solar radiation, which means that SMX was degraded with a higher reaction rate. It can also be noticed that 5%TiO$_2$/LECA had higher values than 3.6%TiO$_2$/LECA, due to more quantity of TiO$_2$ impregnated in this photocatalyst.

Comparing the kinetic constant obtained in the present study with the ones given by Yadav et al (2018), the value obtained was k_{ap} = 0.09 min^{-1} (using 5 g L^{-1} of photocatalyst and 2 L of volume treated, using a UV-C lamp). Thus, the values obtained in the present study are lower (compared to UV-A radiation). This can be explained since UV-C lamps have higher energy to degrade pollutants than UV-A lamps.

5.2.2 Fixed bed reactor
5.2.2.1 Effect of radiation

To compare the two types of radiation, an assay using UV-A radiation and another with solar radiation was made. The configuration used was C$_2$ (Material and methods section) with a flow rate of 0.012 L min^{-1}, using the 3.6%TiO$_2$/LECA. The solar radiation experiment was conducted in the Department of Chemical Engineering of the University of Coimbra. The information regarding the solar experiment is presented in Table 11 and the degradation rates of these two experiments are shown in Figure 19.

Table 11. Solar radiation information, including the maximum and minimum intensity and its energy for 2 hours.

Date	Time	Solar Radiation Intensity (max-min) (W m^{-2})	Energy for 2 hours (kJ m^{-2})
August 18th	1:10-3:10 PM	872-768	6280.5
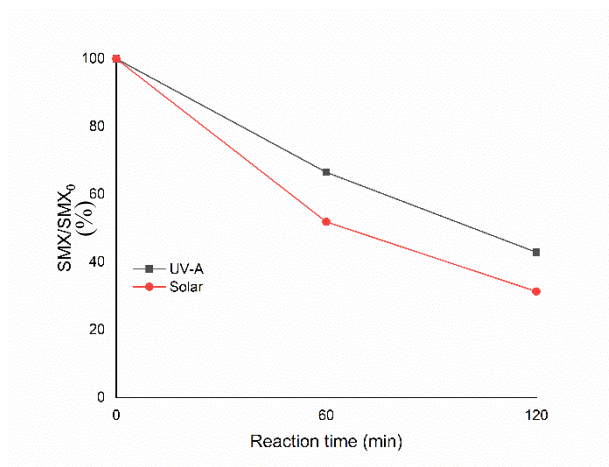
Figure 19. SMX degradation rates for the different radiation types using a flow rate of 0.012 L min^{-1} and the configuration C$_2$.

Analyzing Figure 19, it can be seen that the photocatalysis values for both UV-A and solar radiation are higher than the values of photolysis based in the previous work (Oliveira (2021). Comparing the values from Figure 19, solar radiation removed more SMX from the synthetic effluent (68.7%), while 57.1% of SMX was removed when UV-A radiation was used. Thus, it can be concluded that the reaction under solar light is the most efficient. This can be explained due the range of UV radiation spectrum in the sun's radiation. Having all these wavelengths, the removal of pollutants in the solutions is usually higher.

The mass loss in these reactions was very similar, close to 20%. This percentage is related to the stability of the particles inside the column, which allows a smaller loss of photocatalyst.

Just like previously discussed in the configuration of slurry reactor, the pseudo-first-order kinetic constants for the fixed-bed configuration were also calculated for the two radiations studied. Table 12 resumes this information.

Table 12. Pseudo-first order kinetic constants of the reactions and their R square.

k_{ap} (min^{-1})	
UV-A radiation	**Solar radiation**
0.00698 (0.99964)	0.01016 (0.99286)

As can be seen in Table 12, it can be concluded that by using UV-A radiation, the kinetic constant was lower than when the solar radiation was used. Just like it was mentioned in the slurry configuration, the degradation rates for solar radiation were higher than with UV-A, which explains these results.

In a study conducted by Rao et al (2012) for the decolorization of a reactive dye. Using solar radiation, the kinetic constants were in the range 0.02479 min^{-1} to 0.07858 min^{-1} when a rectangular fixed bed reactor was employed for treating a volume of 660 mL. Since it is a rectangular reactor, the area exposed to radiation was higher, which can explain the better results in that study.

The detention of by-products in the photocatalysis is an important issue since some of them can be more hazardous than the actual pollutant that is being treated, or reduce the degradation rate of the targeted compound.

3-amino-5-methylisoxazole (AMI) and p-benzoquinone (BZQ) were the by-products considered in this thesis. A calibration curve was made for both compounds, in order to determine the quantity that was formed at the end of the reactions (Annex IV). Table 13 shows the concentration of AMI and BZQ for both UV-A and solar radiation for the fixed bed reactor at the end of the reactions.

Table 13. Concentrations of AMI and BZQ, in mg L-1, at the end of the reactions.

Radiation type	AMI concentration (mg L^{-1})	BZQ concentration (mg L^{-1})
UV-A	0.0046	-
Solar	0.0062	-

Considering the values of Table 13, it is clear that AMI was detected in both reaction conditions (with UV-A and solar radiation). However, BZQ, on the other hand, was not detected. These by-products appear due to an attack of the •OH formed during the photocatalysis, on the N-H bond in the SMX structure, forming AMI and sulfanilic acid (SNA) (Zanella et al., 2018). In this way, the 120 min of reaction at these conditions were not enough to produce the BZQ compound for the detection method developed for this by-product.

5.2.2.2   Effect of photocatalyst distribution in reactor

Another aspect that is important to study is the distribution of the photocatalyst throughout the column for the fixed bed configuration, using the same flow rate, to understand if the photocatalyst distributed in the column has a major influence on SMX removal. The four distributions, using a flow rate of 0.012 L min^{-1} and 3.6%TiO$_2$/LECA, were studied using solar radiation. Table 14 displays the details of the different experiments.

Table 14. Experiments with different photocatalyst distribution in the reactor under solar radiation.

Photocatalyst distribution	Date	Time	Solar Radiation Intensity (max-min) (W m^{-2})	Energy for 3 hours (kJ m^{-2})
C_1	July 28th	2:02-5:02 PM	932-171	7981.8
C_2	July 22nd	12:55-3:55 PM	911-742	9570.3
C_3	August 18th	1:10-4:10 PM	872-643	8807.4
C_4	August 19th	1:11-4:11 PM	861-759	8677.2
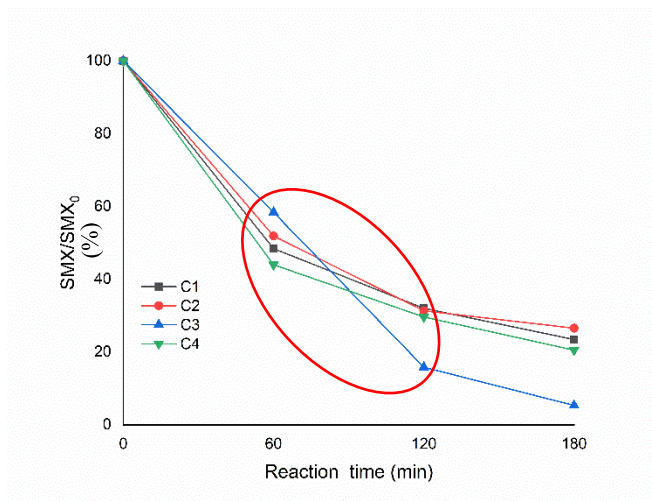
Figure 20. SMX degradation rates for the different photocatalyst distribution in the reactor using a flow rate of 0.012 L min^{-1} for the configurations C_1, C_2, C_3, and C_4.

Comparing the results in Figure 20, after 60 min of reaction, the four configurations have a similar degradation pattern. However, configuration C_3 has a higher degradation rate than the other configurations, between the first and second hour. This happened because the tubes in the recirculation pump leaked, due to high temperatures, leading to a significant

reduction in the volume to be treated. For this reason, configuration C_3 had a higher degradation value, of approximately 94.7%. Considering this, it is recommended to repeat this experiment in the future. Configuration C_1, C_2 and C_4 lead to very similar values, 73.5%, 76.6% and 79.5% of SMX removal after 120 min. However, it was expected that configuration C_1 had better results, due to more photocatalyst dosage introduced in the column. However, considering the solar radiation characteristics on the day that the experiment took place (Annex III), it was observed abrupt radiation peaks, which can explain the lower value compared to the other configurations with less amount of photocatalyst.

5.2.2.3   Effect of flowrate

For the fixed bed reactor configuration, it is relevant to study the flowrate variation, to observe the effect of this operating variable on the degradation results. These experiences used configuration C_1, under solar radiation. Table 15 shows the conditions for the solar radiation experiences and Figure 21 shows the degradation of SMX by photocatalysis

Table 15. Solar radiation details, including the maximum and minimum intensity and its energy for 3 hours.

Flowrate (L min^{-1})	Date	Time	Solar Radiation Intensity (max-min) (W m^{-2})	Energy for 3 hours (kJ m^{-2})
0.006	July 23rd	12:37-3:37 PM	889-761	9592.8
0.012	July 28th	2:02-5:02 PM	932-171	7981.8
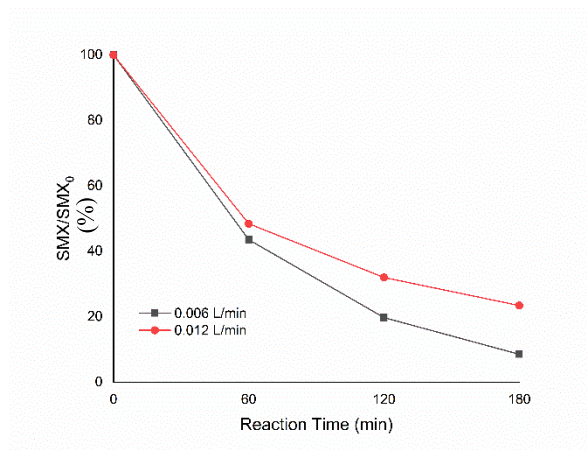
Figure 21. SMX degradation rates for the different radiation types using different flowrates for the configurations C_1.

As can be seen in Figure 21, the degradation rate for the lowest flowrate is higher (91.5%) than for the highest flowrate, (73.5%). It is a conclusion that was expected, since, with lower flowrates, the contact time between the affluent and the photocatalyst supported is higher, removing a higher quantity of pollutants (Borges et al., 2015). Sraw et al (2018) observed that when the recirculation rate increased from 400 to 800 mL min^{-1}, the MCP degradation values had a difference of approximately 12.5%, being the 800 mL^{-1} that had the better results. In the present study, the difference in the removal efficiency between experiments was 21%, a little bit higher compared to the literature. One of the reasons for the difference detected is the less energy, in W m^{-2}, on the day that the reaction using the 0.012 L min^{-1} rate was tested.

The study of the by-product's formation was also made for this effect. Table 16 presents the concentration of AMI and BZQ for both recirculation rates.

Table 16. Concentrations of AMI and BZQ, in mg L-1, at the different reaction times.

Flowrate (L min^{-1})	AMI concentration (mg L^{-1}) 120 min	BZQ concentration (mg L^{-1}) 120 min	AMI concentration (mg L^{-1}) 180 min	BZQ concentration (mg L^{-1}) 180 min
0.006	0.0037	0.0057	0.0022	0.0068
0.012	0.0026	0.0033	-	0.0035

It can be noticed in Table 16 that BZQ is present at the end of these reactions. When confronting the by-products concentration for 120 min and 180 min, it can be seen that AMI

concentration decreases during the reaction and, contrary to this, BZQ increases. Since BZQ has a more complex formation, a higher reaction time allows its production.

Also, it is concluded that AMI concentration was lower than the BZQ, due to their mechanism of formation. Beyond the attack that •OH does to SMX, leading to the production of BZQ, the •OH attacks the amino group and the isoxazole aromatic ring of the AMI and produces BZQ (Zanella et al., 2018). For this reason, BZQ has a higher concentration at the end of the reaction (Zanella et al., 2018).

5.3   Photocatalyst reuse

The photocatalyst reuse using the fixed bed configuration was performed by utilizing the catalyst 3.6% TiO_2/LECA with solar radiation, with the configuration C_1. Between all the cycles, the photocatalyst was not dried, because this procedure improves the efficiency of degradation. Table 17 shows the parameters of both experiments' cycles under solar radiation.

Table 17. Solar radiation details for the three cycles, including the maximum and minimum intensity and its energy for 3 hours.

Cycle	Date	Time	Solar Radiation Intensity (max-min) ($W\ m^{-2}$)	Energy for 2 hours (kJ m^{-2})
1	July 28th	2:02-4:02 PM	932-171	5298.3
2	August 25th	1:56-3:56 PM	819-645	5603.4
3	August 26th	1:17-3:17 PM	810-694	5780.1

After the reactions occurred, it was possible to obtain the degradation values for the 3 cycles. Figure 22 shows the photocatalytic activity differences between cycle 1 to cycle 3.
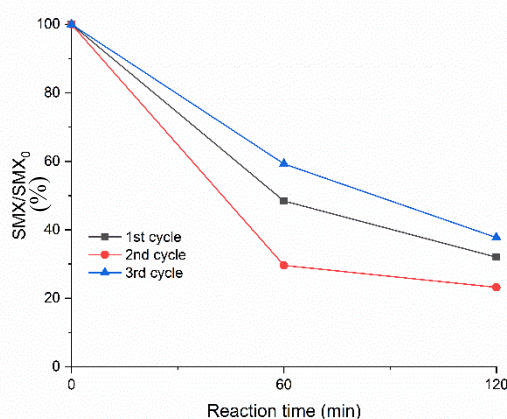
Figure 22. SMX degradation rates for the three cycles using a flow rate of 0.012 L min^{-1} and the configuration C_1.

According to the results shown in Figure 22, the photocatalytic activity had an increase in efficiency in the second cycle, from 68% to 76.8%, while in the third cycle a decrease to 62.3% was observed. This increase between the first and second cycles can be explained by the several TiO_2 layers impregnated in the LECA surface, continuing to have activity sites in the photocatalyst to help in the degradation of SMX. Another possibility is the fact that the solar radiation when the 1st cycle was performed, had peaks during the reaction, having less energy comparing to the energy of the 2nd cycle, leading to a lower degradation efficiency. When the 3rd cycle is performed, there is less quantity of photocatalyst present in the support, leading to a lower efficiency compared to the 1st cycle. Between the second and third cycles, the mass loss was around 20%, which was similar to the previous assays using the fixed bed reactor.

Compared to other studies from the literature using the same reactor configuration, Sraw et al. 2018 observed an efficiency loss of approximately 8% after 30 continuous cycles and Kaur et al. 2018 had a loss of 34% of efficiency at the 40th cycle, which means this experience had good results compared to the other studies made. Thus, in the future, more cycles must be performed to test the catalyst 3.6% TiO_2/LECA.

5.4 Selected conditions

The two configurations studied in this dissertation, slurry reactor, and fixed bed reactor, revealed interesting results, therefore a comparation is required to decide which is the best configuration. To analyze the results of these effects, Table 18 resumes relevant information.

Table 18. Comparison of the best results using slurry and fixed bed reactors.

Reactor configuration	Reaction conditions	Results
Slurry	25 g L^{-1} of TiO_2/LECA, UV-A radiation, air pump, 120 min	Quantity of SMX degraded 5%TiO_2/LECA 53.5%, 63% of TiO_2 lost
	25 g L^{-1} of TiO_2/LECA, solar radiation, air pump, 120 min	Quantity of SMX degraded 5%TiO_2/LECA= 92.3%, 36% of TiO_2 lost
Fixed bed	Configuration C_1, solar radiation, 0.012 L min^{-1}, 120 min	Quantity of SMX degraded 68.9%, 18.9% of TiO_2 loss
	Configuration C_1, solar radiation, 0.006 L min^{-1}, 120 min	Quantity of SMX degraded 80.2%

Analyzing the information given in Table 19, the slurry reactor has better degradation results compared to the fixed bed reactor. Indeed, fixed bed reactor needs to have a higher reaction time, which means higher residence times to have similar degradation rates compared to the slurry reactor. An explanation for this is that the slurry reactor has a large surface area, allowing the particles to receive more radiation when compared to the particles placed in the tubular reactor. Moreover, better dispersion of photocatalysts is obtained during the slurry configuration which allows a higher surface area of photocatalysts available to produce reactive species.

The magnetic stirrer was not considered a good result due to the high nanoparticles of TiO_2 released into the solutions, which is similar to using the photocatalyst as a powder and is not the purpose of this study. However, when it comes to mass loss, is clear that using a fixed bed reactor has better results. This happens because the particles are stable in the reactor, and therefore, they do not have free movement, which leas to less release of TiO_2 supported in LECA or crushing each other.

6. Conclusions and Future Works

The main objective of this dissertation was to evaluate how some parameters could influence the degradation of SMX and to understand which could turn out to be good options when using photocatalysis.

First, the TiO_2 supported in LECA was prepared in two concentrations of TiO_2 impregnated in LECA: 3.6% (w/w) and 5% (w/w). This preparation was provided by previous work, where they were considered the ones who had the better results.

After this preparation, it was tested the best photocatalyst dosage in a slurry reactor, with three different concentrations and a UV-A lamp. It was concluded that the best option was the higher photocatalyst concentration, 25 g L^{-1}, resulting in an SMX elimination of 47.7% for 3.6%TiO_2/LECA and 53.5% for 5%TiO_2/LECA. Compared to a photolysis reaction (15.8% of SMX removal), these results are more attractive. With the photocatalyst dosage selected, the reactor layout effect was tested, having different parameters evaluated for the two reactor configurations: slurry reactor and fixed bed reactor.

For the slurry reactor, aeration and a magnetic stirrer were used when the effect of the mixing system was studied. The magnetic stirrer had the best results having 85% off SMX removal for 3.6%TiO_2/LECA and 73% for 5%TiO_2/LECA. Confronting these results with the mass loss and the reuse of the photocatalysts, it could be seen that the magnetic stirrer promotes a high TiO_2 loss to the solution, and TiO_2 powder has a much more significant effect than that supported.

Another effect studied in this configuration was the radiation type, comparing the degradation rates using a UV-A lamp and solar radiation. It could be concluded that, due to the existence of UV-A and UV-B bands in the sun, the photocatalysis worked better in this system, removing 86% of SMX for 3.6%TiO_2/LECA and 92% for 5%TiO_2/LECA.

Following the parameters evaluated for the slurry reactor, it was tested several effects for the fixed bed reactor. Initially, the radiation type was analyzed, and it was proved that the photocatalysis under solar light had a better result, removing around 69% of SMX within 120 min.

Four different distributions were tested to understand if the positioning of the particles and their quantity of them influenced the degradation rates. The three configurations C_1, C_2, and C_4 had good results at the 180 min reaction, but it was expected that, since the C_1 configuration had more particles in the column, this distribution had a better result than the others (76.6% for C_1 and 79.5% and 73.5% for C_2 and C_4, respectively). This was influenced by the solar radiation that was lower than the radiations for the other configurations.

The last effect of this reactor was the difference in the recirculation rate. It tested two flow rates, 0.006 L min^{-1} and 0.012 L min^{-1}. The lower flowrate lead to SMX removal of 91.5%, which compared to the value of 73.5% for the higher recirculation rate, due to the higher residence time in the reaction, which allows a higher contact time between the SMX and the photocatalyst particles, removing more of this compound.

It also tested the photocatalyst reuse of the fixed bed reactor, to understand how the efficiency of removal differs after more than one cycle of utilization. After the second cycle, the efficiency increased by approximately 8%, and this can be explained because the support could have several layers of TiO$_2$ impregnated in it and for that reason, the active sites did not decrease in this reaction. Another explanation could be the lower energy of the solar radiation in the day that the 1st occurred. When it was made the third cycle, the degradation of SMX was 62%, which can be concluded that there were fewer TiO$_2$ particles activated, reducing the removal of this antibiotic.

In the end, it were evaluated all these effects for the two reactor configurations, selecting the ones which had the better results. In general, the slurry reactor had better degradation results, due to having a larger surface area, allowing the particles to receive more radiation. In terms of TiO$_2$ loss during the reaction, the fixed bed reactor had losses of approximately 20% for most of the experiences and, in the best option for the slurry, the loss was 63%. In the fixed bed reactor, the particles are stable in the reactor, which decreases the erosion of the photocatalyst.

Having all this information in account, it can be proved that these two reactor configurations have the potential for the degradation of SMX, but the fixed bed reactor was the one who lost less TiO$_2$ and had good degradation values

However, there are still some studies that should be made to complement the results that this dissertation showed, for example:

1. Studying more effects in the reactors, like the flow rate of the air pump and the velocity of the magnetic stirrer, for different SMX concentrations;
2. Testing the same reactor configuration with different dimensions, to understand how this parameter can influence the degradation rate since that can be possible to enhance the area available to the photocatalyst to absorb radiation;
3. Do these tests with more CEC, to compare their degradation results with each other;
4. Analyze more by-products that can appear during the photocatalysis of SMX;
5. Perform ecotoxicity tests to evaluate if the treated solutions presented lower toxicity compared to the initial solutions.

References

Abbaspour, K. C., Faramarzi, M., Ghasemi, S. S., & Yang, H. (2009). Assessing the impact of climate change on water resources in Iran. *Water Resources Research*, *45*(10), 1–16. https://doi.org/10.1029/2008WR007615

Abhang, R. M., Kumar, D., & Taralkar, S. V. (2011). Design of Photocatalytic Reactor for Degradation of Phenol in Wastewater. *International Journal of Chemical Engineering and Applications*, *2*(5), 337–341. https://doi.org/10.7763/ijcea.2011.v2.130

Ahmad, A. L., Chin, J. Y., Mohd Harun, M. H. Z., & Low, S. C. (2022). Environmental impacts and imperative technologies towards sustainable treatment of aquaculture wastewater: A review. *Journal of Water Process Engineering*, *46*, 1–13. https://doi.org/10.1016/j.jwpe.2021.102553

Al-Taweel, S. S., & Saud, H. R. (2016). New route for synthesis of pure anatase TiO2 nanoparticles via utrasound-assisted sol-gel method. *Journal of Chemical and Pharmaceutical Research*, *8*(2), 620–626.

Ameta, R., Solanki, M. S., Benjamin, S., & Ameta, S. C. (2018). Photocatalysis. In *Advanced Oxidation Processes for Wastewater Treatment* (1st ed., pp. 135–175). Academic Press. https://doi.org/10.1016/B978-0-12-810499-6.00006-1

Balasubramanian, R., Brar, S., Hamilton, A., Klein, E., & Boeckel, T. Van. (2021). *The State of the World's Antibiotics 2021 A Global Analysis of Antimicrobial Resistance and Its Drivers*.

Baralla, E., Demontis, M. P., Dessì, F., & Varoni, M. V. (2021). An overview of antibiotics as emerging contaminants: Occurrence in bivalves as biomonitoring organisms. *Animals*, *11*(11), 1–17. https://doi.org/10.3390/ani11113239

Barnes, K. K., Kolpin, D. W., Furlong, E. T., Zaugg, S. D., Meyer, M. T., & Barber, L. B. (2008). A national reconnaissance of pharmaceuticals and other organic wastewater contaminants in the United States - I) Groundwater. *Science of the Total Environment*, *402*((2-3)), 192–200. https://doi.org/10.1016/j.scitotenv.2008.04.028

Batt, A. L., Kim, S., & Aga, D. S. (2007). Comparison of the occurrence of antibiotics in four full-scale wastewater treatment plants with varying designs and operations. *Chemosphere*, *68*(3), 428–435. https://doi.org/10.1016/j.chemosphere.2007.01.008

Borges, M. E., García, D. M., Hernández, T., Ruiz-Morales, J. C., & Esparza, P. (2015). Supported photocatalyst for removal of emerging contaminants from wastewater in a

continuous packed-bed photoreactor configuration. *Catalysts*, *5*(1), 77–87. https://doi.org/10.3390/catal5010077

Bottoni, P., Caroli, S., & Caracciolo, A. B. (2010). Pharmaceuticals as priority water contaminants. *Toxicological and Environmental Chemistry*, *92*(3), 549–565. https://doi.org/10.1080/02772241003614320

Bouchy, M., & Zahraa, O. (2003). Photocatalytic reactors. *International Journal of Photoenergy*, *5*(3), 191–197. https://doi.org/10.1155/S1110662X03000321

Brown, K. D., Kulis, J., Thomson, B., Chapman, T. H., & Mawhinney, D. B. (2006). Occurrence of antibiotics in hospital, residential, and dairy effluent, municipal wastewater, and the Rio Grande in New Mexico. *Science of the Total Environment*, *366*((2-3)), 772–783. https://doi.org/10.1016/j.scitotenv.2005.10.007

Brumovský, M., Bečanová, J., Kohoutek, J., Borghini, M., & Nizzetto, L. (2017). Contaminants of emerging concern in the open sea waters of the Western Mediterranean. *Environmental Pollution*, *229*(1), 976–983. https://doi.org/10.1016/j.envpol.2017.07.082

Carvalho, I. T., & Santos, L. (2016). Antibiotics in the aquatic environments : A review of the European scenario. *Environment International*, *94*, 736–757. https://doi.org/10.1016/j.envint.2016.06.025

Černigoj, U., Štangar, U. L., & Trebše, P. (2007). Evaluation of a novel Carberry type photoreactor for the degradation of organic pollutants in water. *Journal of Photochemistry and Photobiology A: Chemistry*, *188*(2–3), 169–176. https://doi.org/10.1016/j.jphotochem.2006.12.009

Chaplin, M. F. (2001). Water: its importance to life. *Biochemistry and Molecular Biology Education*, *29*, 54–59.

Chirwa, E., & Bamuza-Pemu, E. (2010). Investigation of photocatalysis as an alternative to other advanced oxidation processes for the treatment of filter backwash water. In *WRC Report*. https://doi.org/10.13140/RG.2.1.1368.3042

Danfá, S., Martins, R. C., Quina, M. J., & Gomes, J. (2021). Supported tio2 in ceramic materials for the photocatalytic degradation of contaminants of emerging concern in liquid effluents: A review. *Molecules*, *26*(17), 1–27. https://doi.org/10.3390/molecules26175363

Commission Implementing Decision (EU) 2022/1307, establishng a atch list of substances for Union-wide monitoring in the field of water policy pursuant to Directive 2008/105/EC of the European Parliament and of the Council (2022) OJ L197/117.

Dong, H., Zeng, G., Tang, L., Fan, C., Zhang, C., He, X., & He, Y. (2015). An overview on limitations of TiO2-based particles for photocatalytic degradation of organic pollutants and the corresponding countermeasures. *Water Research*, *79*, 128–146.

https://doi.org/10.1016/j.watres.2015.04.038

Ferreira, S. H., Morais, M., Nunes, D., Oliveira, M. J., Rovisco, A., Pimentel, A., Águas, H., Fortunato, E., & Martins, R. (2021). High UV and sunlight photocatalytic performance of porous ZnO nanostructures synthesized by a facile and fast microwave hydrothermal method. *Materials*, *14*(9), 1–17. https://doi.org/10.3390/ma14092385

Gaffney, V., Cardoso, V. V., Cardoso, E., Teixeira, A. P., Martins, J., Benoliel, M. J., & Almeida, C. M. M. (2017). Occurrence and behaviour of pharmaceutical compounds in a Portuguese wastewater treatment plant: Removal efficiency through conventional treatment processes. *Environmental Science and Pollution Research*, *24*(17), 14717–14734. https://doi.org/10.1007/s11356-017-9012-7

Gorde, S. P., & Jadhav, M. V. (2013). Assessment of Water Quality Parameters : A Review. *International Journal of Engineering Research and Applications*, *3*(6), 2029–2035.

Hossain, A., Nakamichi, S., Habibullah-Al-Mamun, M., Tani, K., Masunaga, S., & Matsuda, H. (2018). Occurrence and ecological risk of pharmaceuticals in river surface water of Bangladesh. *Environmental Research*, *165*(1), 258–266. https://doi.org/10.1016/j.envres.2018.04.030

Hossain, M. F. (2019). Water. In *Sustainable Design and Build: Building, Energy, Roads, Bridges, Water and Swer Systems* (1st ed., pp. 301–418). Butterworth-Heinemann. https://doi.org/10.1016/B978-0-12-816722-9.00006-9

Inglezakis, V. J., & Poulopoulos, S. G. (2006). Heterogeneous Processes and Reactor Analysis. In *Adsorption, Ion Exchange and Catalysis Design of Operations and Environmental Applications* (1st ed., pp. 57–242). Elsevier Science. https://doi.org/10.1016/b978-044452783-7/50003-3

Jendrzejewska, N., & Karwowska, E. (2018). The influence of antibiotics on wastewater treatment processes and the development of antibiotic-resistant bacteria. *Water Science & Technology*, *77*(9), 2320–2326. https://doi.org/10.2166/wst.2018.153

Jiménez, M., Ignacio Maldonado, M., Rodríguez, E. M., Hernández-Ramírez, A., Saggioro, E., Carra, I., & Sánchez Pérez, J. A. (2015). Supported TiO2 solar photocatalysis at semi-pilot scale: Degradation of pesticides found in citrus processing industry wastewater, reactivity and influence of photogenerated species. *Journal of Chemical Technology and Biotechnology*, *90*(1), 149–157. https://doi.org/10.1002/jctb.4299

Johnson, A. C., Keller, V., Dumont, E., & Sumpter, J. P. (2015). Assessing the concentrations and risks of toxicity from the antibiotics ciprofloxacin, sulfamethoxazole, trimethoprim and erythromycin in European rivers. *Science of the Total Environment*, *511*, 747–755. https://doi.org/10.1016/j.scitotenv.2014.12.055

Kaur, T., Sraw, A., Wanchoo, R. K., & Toor, A. P. (2018). Solar assisted degradation of carbendazim in water using clay beads immobilized with TiO2 & Fe doped TiO2. *Solar Energy*, *162*(1), 45–56. https://doi.org/10.1016/j.solener.2017.11.033

Lester, Y., Avisar, D., & Mamane, H. (2010). Photodegradation of the antibiotic sulphamethoxazole in water with UV/H2O2 advanced oxidation process. *Environmental Technology*, *31*(2), 175–183. https://doi.org/10.1080/09593330903414238

Long, Z., Li, Q., Wei, T., Zhang, G., & Ren, Z. (2020). Historical development and prospects of photocatalysts for pollutant removal in water. *Journal of Hazardous Materials*, *395*, 1–27. https://doi.org/10.1016/j.jhazmat.2020.122599

López-Serna, R., Jurado, A., Vázquez-Suñé, E., Carrera, J., Petrović, M., & Barceló, D. (2013). Occurrence of 95 pharmaceuticals and transformation products in urban groundwaters underlying the metropolis of Barcelona, Spain. *Environmental Pollution*, *174*, 305–315. https://doi.org/10.1016/j.envpol.2012.11.022

Manassero, A., Satuf, M. L., & Alfano, O. M. (2017). Photocatalytic reactors with suspended and immobilized TiO2: Comparative efficiency evaluation. *Chemical Engineering Journal*, *326*, 29–36. https://doi.org/10.1016/j.cej.2017.05.087

Martini, J., Orge, C. A., Faria, J. L., Pereira, M. F. R., & Soares, O. S. G. P. (2019). Catalytic advanced oxidation processes for sulfamethoxazole degradation. *Applied Sciences*, *9*(13), 1–18. https://doi.org/10.3390/app9132652

McCullagh, C., Skillen, N., Adams, M., & Robertson, P. K. J. (2011). Photocatalytic reactors for environmental remediation: A review. *Journal of Chemical Technology and Biotechnology*, *86*(8), 1002–1017. https://doi.org/10.1002/jctb.2650

Mestre, A. S., & Carvalho, A. P. (2019). Photocatalytic Degradation of Pharmaceuticals Wastewater. *Molecules*, *24*, 3702. https://www.mdpi.com/1420-3049/24/20/3702/pdf

Mohapatra, S., Huang, C. H., Mukherji, S., & Padhye, L. P. (2016). Occurrence and fate of pharmaceuticals in WWTPs in India and comparison with a similar study in the United States. *Chemosphere*, *159*, 526–535. https://doi.org/10.1016/j.chemosphere.2016.06.047

Monfort, O., & Petrisková, P. (2021). Binary and Ternary Vanadium Oxides: General Overview, Physical Properties, and Photochemical Processes for Environmental Applications. *Processes*, *9*(214), 5–61. https://doi.org/10.3390/pr9112080

Nilsen, E., Smalling, K. L., Ahrens, L., Gros, M., Miglioranza, K. S. B., Picó, Y., & Schoenfuss, H. L. (2019). Critical review: Grand challenges in assessing the adverse effects of contaminants of emerging concern on aquatic food webs. *Environmental Toxicology and Chemistry*, *38*(1), 46–60. https://doi.org/10.1002/etc.4290

Oliveira, C. (2021). *Remoção De Contaminantes Orgânicoa De Efluentes Líquidos Por*

Processo De Fotocatálise. Universidade de Coimbra.

Pastorino, P., & Ginebreda, A. (2021). Contaminants of emerging concern (CECs): Occurrence and fate in aquatic ecosystems. *International Journal of Environmental Research and Public Health*, *18*(24), 18–21. https://doi.org/10.3390/ijerph182413401

Perry, R. H., Green, D. W., & Maloney, J. O. (1997). Perry's Chemical Engineer ' Handbook. In *Society* (7th ed.). McGraw-Hill.

Peters, R. F., Dos Santos, P. A. M., Machado, T. C., Lopez, D. A. R., Machado, Ê. L., & De Assis Lawisch Rodriguez, A. (2018). Photocatalytic degradation of methylene blue using TiO2 supported in ceramic material. *Eclética Quimica Journal*, *43*(1), 26–32. https://doi.org/10.26850/1678-4618eqj.v43.1.26-32

Prasannamedha, G., & Kumar, P. S. (2020). A review on contamination and removal of sulfamethoxazole from aqueous solution using cleaner techniques : Present and future perspective. *Journal of Cleaner Production*, *250*(1), 2–8. https://doi.org/10.1016/j.jclepro.2019.119553

Pubchem. (2022a). *Sulfamethoxazole*. https://pubchem.ncbi.nlm.nih.gov/compound/Sulfamethoxazole#section=Names-and-Identifiers

Pubchem. (2022b). *Titanium dioxide / TiO2 - PubChem*. https://pubchem.ncbi.nlm.nih.gov/compound/Titanium-dioxide#section=Computed-Properties

Pulicharla, R., Proulx, F., Behmel, S., Sérodes, J. B., & Rodriguez, M. J. (2021). Occurrence and seasonality of raw and drinking water contaminants of emerging interest in five water facilities. *Science of the Total Environment*, *751*, 1–11. https://doi.org/10.1016/j.scitotenv.2020.141748

Rao, N. N., Chaturvedi, V., & Li Puma, G. (2012). Novel pebble bed photocatalytic reactor for solar treatment of textile wastewater. *Chemical Engineering Journal*, *184*, 90–97. https://doi.org/10.1016/j.cej.2012.01.004

Rashad, A. M. (2018). Lightweight expanded clay aggregate as a building material – An overview. *Construction and Building Materials*, *170*, 757–775. https://doi.org/10.1016/j.conbuildmat.2018.03.009

Ren, G., Han, H., Wang, Y., Liu, S., Zhao, J., Meng, X., & Li, Z. (2021). Recent advances of photocatalytic application in water treatment: A review. *Nanomaterials*, *11*(7), 1–22. https://doi.org/10.3390/nano11071804

Rivera-Utrilla, J., Sánchez-Polo, M., Ferro-García, M. Á., Prados-Joya, G., & Ocampo-Pérez, R. (2013). Pharmaceuticals as emerging contaminants and their removal from water. A

review. *Chemosphere*, *93*(7), 1268–1287. https://doi.org/10.1016/j.chemosphere.2013.07.059

Sacco, O., Sannino, D., & Vaiano, V. (2019). Packed bed photoreactor for the removal of water pollutants using visible light emitting diodes. *Applied Sciences*, *9*(472), 1–14. https://doi.org/10.3390/app9030472

Sacher, F., Lange, F. T., Brauch, H. J., & Blankenhorn, I. (2001). Pharmaceuticals in groundwaters: Analytical methods and results of a monitoring program in Baden-Württemberg, Germany. *Journal of Chromatography A*, *938*(1), 199–210. https://doi.org/10.1016/S0021-9673(01)01266-3

Salimi, M., Esrafili, A., Gholami, M., Jonidi Jafari, A., Rezaei Kalantary, R., Farzadkia, M., Kermani, M., & Sobhi, H. R. (2017). Contaminants of emerging concern: a review of new approach in AOP technologies. *Environmental Monitoring and Assessment*, *189*(414), 1–22. https://doi.org/10.1007/s10661-017-6097-x

Sarni, W., & Grant, D. (2021). Valuing Water. In *The United Nations World Water Development Report 2021*. https://doi.org/10.4324/9781315627250-3

Sharma, S., & Bhattacharya, A. (2017). Drinking water contamination and treatment techniques. *Applied Water Science*, *7*(3), 1043–1067. https://doi.org/10.1007/s13201-016-0455-7

Shavisi, Y., Sharifnia, S., Hosseini, S. N., & Khadivi, M. A. (2014). Application of TiO2/perlite photocatalysis for degradation of ammonia in wastewater. *Journal of Industrial and Engineering Chemistry*, *20*, 278–283. https://doi.org/10.1016/j.jiec.2013.03.037

Shavisi, Y., Sharifnia, S., Zendehzaban, M., Mirghavami, M. L., & Kakehazar, S. (2014). Application of solar light for degradation of ammonia in petrochemical wastewater by a floating TiO2/LECA photocatalyst. *Journal of Industrial and Engineering Chemistry*, *20*(5), 2806–2813. https://doi.org/10.1016/j.jiec.2013.11.011

Sim, W. J., Lee, J. W., Lee, E. S., Shin, S. K., Hwang, S. R., & Oh, J. E. (2011). Occurrence and distribution of pharmaceuticals in wastewater from households, livestock farms, hospitals and pharmaceutical manufactures. *Chemosphere*, *82*(2), 179–186. https://doi.org/10.1016/j.chemosphere.2010.10.026

Sraw, A., Kaur, T., Pandey, Y., Sobti, A., Wanchoo, R. K., & Toor, A. P. (2018). Fixed bed recirculation type photocatalytic reactor with TiO2 immobilized clay beads for the degradation of pesticide polluted water. *Journal of Environmental Chemical Engineering*, *6*(6), 7035–7043. https://doi.org/10.1016/j.jece.2018.10.062

Stanhill, G. (1986). Water use efficiency. In *Advances in Agronomy* (1st ed., Vol. 39, pp. 53–85). Academic Press. https://doi.org/10.1016/S0065-2113(08)60465-4

Varela, A. R., André, S., Nunes, O. C., & Manaia, C. M. (2014). Insights into the relationship between antimicrobial residues and bacterial populations ina hospital-urban wastewater treatment plant system. *Water Research*, *54*, 327–336. https://doi.org/10.1016/j.watres.2014.02.003

Vidal-Dorsch, D. E., Bay, S. M., Maruya, K., Snyder, S. A., Trenholm, R. A., & Vanderford, B. J. (2012). Contaminants of emerging concern in municipal wastewater effluents and marine receiving water. *Environmental Toxicology and Chemistry*, *31*(12), 2674–2682. https://doi.org/10.1002/etc.2004

VO, P., Ngo, H. H., Guo, W., Zhou, J. L., Nguyen, P. D., Listowski, A., & Wang, X. C. (2014). A mini-review on the impacts of climate change on wastewater reclamation and reuse. *Science of the Total Environment*, *494–495*, 9–17. https://doi.org/10.1016/j.scitotenv.2014.06.090

Watkinson, A. J., Murby, E. J., & Costanzo, S. D. (2007). Removal of antibiotics in conventional and advanced wastewater treatment: Implications for environmental discharge and wastewater recycling. *Water Research*, *41*(18), 4164–4176. https://doi.org/10.1016/j.watres.2007.04.005

Welty, J. R., Wickes, C. E. W., Wilson, R. E., & Rorrer, G. L. (2008). *Fundamentals of Momentum, Heat, and Mass Transferr* (5th ed.). John Wiley & Sons, Inc.

Xu, W. hai, Zhang, G., Zou, S. chun, Li, X. dong, & Liu, Y. chun. (2007). Determination of selected antibiotics in the Victoria Harbour and the Pearl River, South China using high-performance liquid chromatography-electrospray ionization tandem mass spectrometry. *Environmental Pollution*, *145*(3), 672–679. https://doi.org/10.1016/j.envpol.2006.05.038

Yadav, D., Rangabhashiyam, S., Verma, P., Singh, P., Devi, P., Kumar, P., Hussain, C. M., Gaurav, G. K., & Kumar, K. S. (2021). Environmental and health impacts of contaminants of emerging concerns: Recent treatment challenges and approaches. *Chemosphere*, *272*, 1–19. https://doi.org/10.1016/j.chemosphere.2020.129492

Yadav, M. S., Neghi, N., Kumar, M., & Varghese, G. K. (2018). Photocatalytic-oxidation and photo-persulfate-oxidation of sulfadiazine in a laboratory-scale reactor: Analysis of catalyst support, oxidant dosage, removal-rate and degradation pathway. *Journal of Environmental Management*, *222*, 164–173. https://doi.org/10.1016/j.jenvman.2018.05.052

Yasmina, M., Mourad, K., Mohammed, S. H., & Khaoula, C. (2014). Treatment heterogeneous photocatalysis; Factors influencing the photocatalytic degradation by TiO2. *Energy Procedia*, *50*, 559–566. https://doi.org/10.1016/j.egypro.2014.06.068

Zanella, R., Avella, E., Ramírez-Zamora, R. M., Castillón-Barraza, F., & Durán-Álvarez, J. C.

(2018). Enhanced photocatalytic degradation of sulfamethoxazole by deposition of Au, Ag and Cu metallic nanoparticles on TiO2. *Environmental Technology (United Kingdom)*, *39*(18), 2353–2364. https://doi.org/10.1080/09593330.2017.1354926

Zdarta, J., Degórska, O., Jankowska, K., Rybarczyk, A., Piasecki, A., Ciesielczyk, F., & Jesionowski, T. (2022). Removal of persistent sulfamethoxazole and carbamazepine from water by horseradish peroxidase encapsulated into poly(Vinyl chloride) electrospun fibers. *International Journal of Molecular Sciences*, *23*(272), 1–16. https://doi.org/10.3390/ijms23010272

Zendehzaban, M., Sharifnia, S., & Hosseini, S. N. (2013). Photocatalytic degradation of ammonia by light expanded clay aggregate (LECA)-coating of TiO2 nanoparticles. *Korean Journal of Chemical Engineering*, *30*(3), 574–579. https://doi.org/10.1007/s11814-012-0212-z

Zimmerman, J. B., Mihelcic, J. R., & Smith, J. (2008). Global Stressors on Water Quality and Quantity. *Enviromental Science and Technology*, *42*(12), 4247–4254.

Annexs

Annex I – TiO$_2$ impregnation in LECA

I.1 TiO$_2$ impregnation in LECA

The procedure followed, since the preparation of LECA and the TiO$_2$ suspension to the impregnation of TiO$_2$ into the LECA was based on a previous work, where all the parameters were tested, reaching the methods described below (Oliveira, 2021).

I.1.1 Preparation of LECA particles

To use LECA in this study, it is necessary to wash it first, to remove undesirable particles. This process started with washing LECA particles in a metal basket with water for about 10 seconds. In this way, larger particles are removed from the catalytic support. After this step, LECA is placed in a 2 L container, and it is manually agitated. It is necessary to be careful to not cause friction within the LECA particles. After this procedure, waits 10 min to remove the LECA particles that are floating, and those are placed again in the 2 L container with clean water. This procedure is done 3 times, to make sure the LECA particles are clean. Following this step, LECA is placed in several glasses and is dried on a stove at 105ºC, for at least 24 h. Finally, LECA is sifted to have the diameter wanted, between 3.36-4.76 mm.

I.1.2 Preparation of TiO$_2$ suspension

For this study, it was made a dispersion of 500 and 710 mg of TiO2 (3.6% and 5% w/w of TiO$_2$, in that order) in 18 mL of ethanol and 1.5 mL of HNO$_3$ which is diluted at 10%. To disperse the suspension, ultrasounds are used for 30 min.

I.1.3 Impregnation of TiO$_2$ suspension in LECA particles

After the dispersion of TiO$_2$ in ultrasounds, 10 g of LECA are placed in the suspension and goes into the ultrasounds for 15 min. At the end of this procedure, the impregnated LECA is dried at 105ºC in the oven for 15h. The next step is to calcinate the particles of LECA, for 30 min at 550ºC. The particles are placed in porcelain melting pots. Finished the calcination step, the samples are weighted, to observe the mass loss of TiO$_2$ from LECA particles during the washing step. To remove the excess of TiO$_2$ in the samples, they are washed and placed again on the stove at 105ºC for 15h. finally, the samples are weighted to see the incorporated TiO$_2$ mass in the support. Equation I demonstrated this calculation.

$$m_{TiO_2 incorporated} = m_f - m_i \qquad \text{(I)}$$

Where $m_{TiO_2 incorporated}$ is the quantity of TiO_2 that is impregnated in LECA, in g, m_f is the mass of LECA plus TiO_2 impregnated at the end of the incorporation, in g, and m_i is the mass of LECA without TiO_2, ie, at the beginning of the impregnation in the support, in g.

I.2 TiO$_2$ Efficiency of TiO$_2$ impregnation in LECA

The efficiencies of TiO_2 impregnation are shown in Table I. The assays using the slurry reactor used a quantity of 16.72 mg$_{TiO2}$/g$_{LECA}$ and for the fixed bed, the quantity was 19.53 mg$_{TiO2}$/g$_{LECA}$ due to the necessity of preparing more particles.

Table 19. Quantity of TiO2 impregnated for the different photocatalysts used.

Photocatalyst	Mean (mg$_{TiO2}$/LECA)	Standard deviation
3.6% TiO$_2$/LECA	16.72	2.54
5% TiO$_2$/LECA	22.31	4.26
3.6% TiO$_2$/LECA - refill	19.53	2.09

Annex II – Regime determination

The determination of the regime type of the flowrates used in this thesis, 0.012 L min^{-1} and 0.006 L min^{-1} comes, in the first place, with the calculation of the interstitial velocity, u_i. This is given by the Equation II (Welty et al., 2008).

$$Q = u_i \, \varepsilon_v \, A \tag{II}$$

Where Q is the recirculation feed, in $m^3 \, s^{-1}$, ε_v is the volumetric porosity and A is the surface area, in m^2. The ε_v was calculated with relation between the column volume when is empty and the volume of the column with the bed.

Having the values of u_i, it can be calculated the Reynolds number (Re), given by Equation III.

$$Re = \frac{\rho \, u_i \, d}{\mu} \tag{III}$$

Where ρ is density of the fluid, in kg m^{-3}, that was considered equal to the water density at 25ºC, d is the column diameter and μ is the viscosity of the fluid, also considered equal to the water at 25ºC, in Pa.s (Perry et al., 1997) .

After this calculation, the values of Re are shown in Table II.

Table 20. Recirculation rates used in this study and their respective Re.

Flowrate (L min^{-1})	Re
0.006	28.3
0.012	57.1

Since Re < 2000, it can be concluded that both flowrates used in this study are considered laminar.
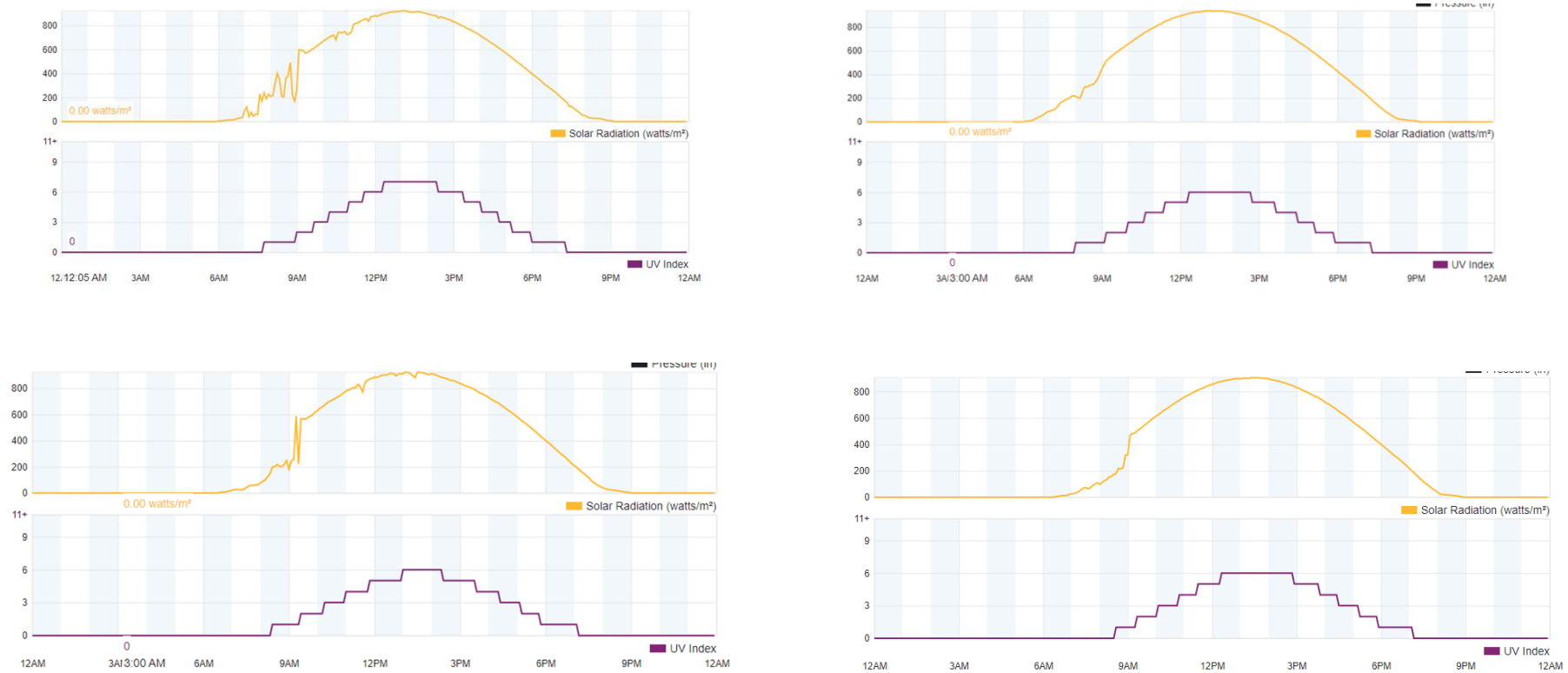
Annex III – Solar radiation details

Figure 23. Solar radiation diagrams at Polo 1 of the University of Coimbra a a) June 9th b) June 28th c) July 22nd d) July 23rd e) July 28th f) August 18th g) August 19th h) August 25th i) August 26th.
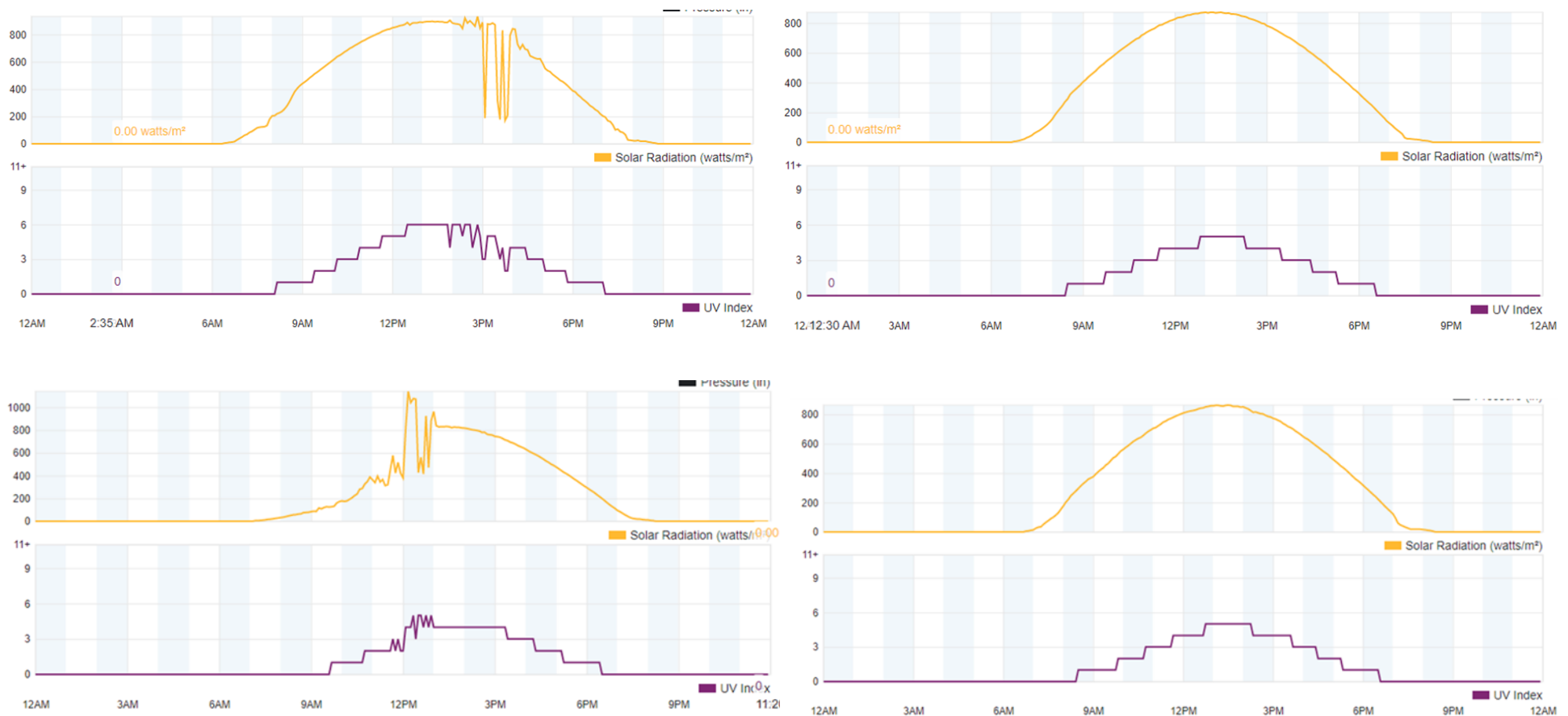
Figure III. Solar radiation diagrams at Polo 1 of the University of Coimbra a a) June 9th b) June 28th c) July 22nd d) July 23rd e) July 28th f) August 18th g) August 19th h) August 25th i) August 26th.
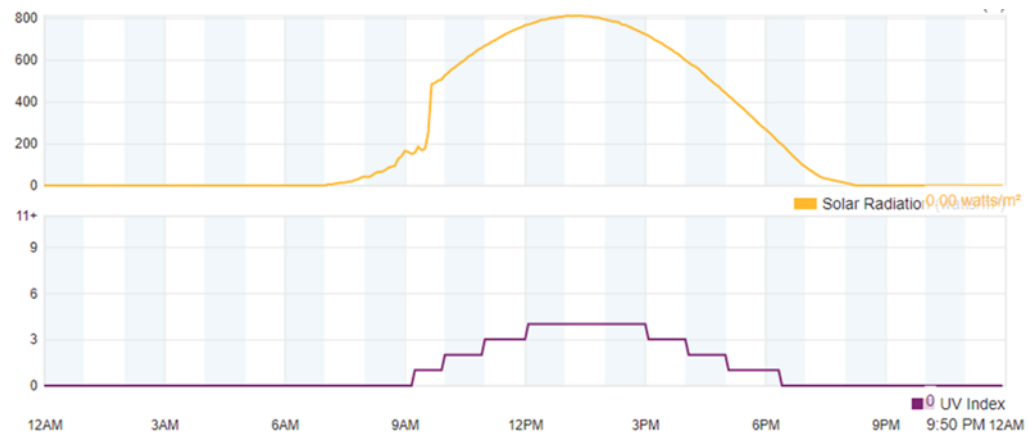
Figure III. Solar radiation diagrams at Polo 1 of the University of Coimbra a a) June 9th b) June 28th c) July 22nd d) July 23rd e) July 28th f) August 18th g) August 19th h) August 25th i) August 26th.
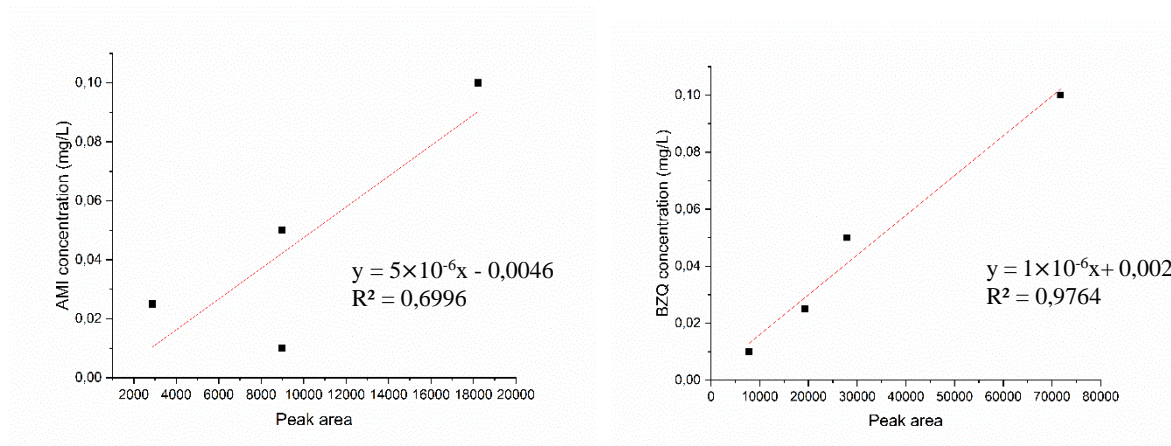
Annex IV – By-products calibration curves

Figure 24 . a) AMI calibration curve and linear equation b) BZQ calibration curve and linear equation.